Palaeoclimatic oscillations in the Pliensbachian (Early Jurassic) of the Asturian Basin (Northern Spain).

J.J. Gómez[1], M.J. Comas-Rengifo[2] and A. Goy[3]

[1] Departmento de Estratigrafía, Facultad de Ciencias Geológicas (UCM) and Instituto de Geociencias (CSIC-UCM). 28040 Madrid. Spain

[2] Departmento de Paleontología, Facultad de Ciencias Geológicas (UCM). 28040 Madrid. Spain

[3] Departmento de Paleontología, Facultad de Ciencias Geológicas (UCM) and Instituto de Geociencias (CSIC-UCM). 28040 Madrid. Spain

Correspondence to: jgomez@ucm.es

Abstract.

One of the main controversial items in palaeoclimatology is to elucidate if climate during the Jurassic was warmer than present day, with no ice caps, or if ice caps were present in some specific intervals. The Pliensbachian Cooling event (Early Jurassic) has been pointed out as one of the main candidates to have developed ice caps on the poles. To constrain the timing of this cooling event, including the palaeoclimatic evolution before and after cooling, as well as the calculation of the seawater palaeotemperatures are of primary importance to find arguments on this subject. For this purpose, the Rodiles section of the Asturian Basin (Northern Spain), a well exposed succession of the uppermost Sinemurian, Pliensbachian and Lower Toarcian deposits, has been studied. A total of 562 beds were measured and sampled for ammonites, for biochronostratigraphical purposes and for belemnites, to determine the palaeoclimatic evolution through stable isotope studies. Comparison of the recorded latest Sinemurian, Pliensbachian and Early Toarcian changes in seawater palaeotemperature with other European sections allows characterization of several climatic changes of probable global extent. A warming interval which partly coincides with a $\delta^{13}C_{bel}$ negative excursion was recorded at the Late Sinemurian. After a "normal" temperature interval, a new warming interval that contains a short lived positive $\delta^{13}C_{bel}$ peak, was developed at the Early–Late Pliensbachian transition. The Late Pliensbachian represents an outstanding cooling interval containing a $\delta^{13}C_{bel}$ positive excursion interrupted by a small negative $\delta^{13}C_{bel}$ peak. Finally, the Early Toarcian represented an exceptional warming period pointed as the main responsible for the prominent Early Toarcian mass extinction.

1 Introduction

The idea of an equable Jurassic greenhouse climate, 5–10º C warmer than present day, with no ice caps and low pole-equator temperature gradient, has been proposed by several studies (i.e. Hallam, 1975, 1993; Chandler et al., 1992; Frakes et al., 1992; Rees et al., 1999; Sellwood and Valdes, 2008). Nevertheless, this hypothesis has been challenged by numerous palaeoclimatic studies, mainly based on palaeotemperature calculations using the oxygen isotope data from belemnite and brachiopod calcite as a proxy. Especially relevant are the latest Pliensbachian−Early Toarcian climate changes, which have been documented in many sections from Western Europe (i. e. Sælen et al., 1996; McArthur et al., 2000; Röhl et al., 2001; Schmidt-Röhl et al., 2002; Bailey et al., 2003; Jenkyns, 2003; Rosales et al., 2004; Gómez et al., 2008; Metodiev and Koleva-Rekalova, 2008; Suan et al., 2008, 2010; Dera et al., 2009, 2010, 2011; Gómez and Arias, 2010; García Joral et al., 2011; Gómez and Goy, 2011; Fraguas et al., 2012), as well as in Northern Siberia and in the Artic Region (Zakharov et al., 2006; Nikitenko, 2008; Suan et al., 2011). The close correlation between the severe Late Pliensbachian Cooling and the Early Toarcian Warming events, and the major Early Toarcian mass extinction indicates that warming was one of the main causes of the faunal turnover (Kemp et al., 2005; Gómez et al., 2008; Gómez and Arias, 2010; García Joral et al., 2011; Gómez and Goy, 2011; Fraguas et al., 2012; Clémence, 2014; Clémence et al., 2015; Baeza-Carratalá et al., 2015).

Comparison between the $\delta^{18}O$-derived palaeotemperature curves obtained from belemnite calcite in the European sections shows a close relationship in the evolution of seawater palaeotemperature across Europe, indicating that the Late Pliensbachian cooling and the Early Toarcian warming intervals could probably be global in extent. At the Late Pliensbachian Cooling event, palaeotemperatures of around 10ºC have been calculated for the Paris Basin (Dera et al., 2009) and in the order of 12ºC for Northern Spain (Gómez et al., 2008; Gómez and Goy, 2011). These temperatures are considerably low for a palaeolatitude of Iberia of around 30–35º N (Osete et al., 2010). Nevertheless, except for a few sections (Rosales et al., 2004; Korte and Hesselbo, 2011; Armendáriz et al., 2012), little data on the evolution of seawater palaeotemperatures during the latest Sinemurian and the Pliensbachian, which culminated in the prominent Late Pliensbachian Cooling and the Early Toarcian Warming events, have been documented.

The objective of this paper is to provide data on the evolution of the seawater palaeotemperatures and the changes in the carbon isotopes through the Early Jurassic Late Sinemurian, Pliensbachian and Early Toarcian, to constrain the timing of the recorded changes through ammonite-based chronostratigraphy. The dataset has been obtained from the particularly well exposed Rodiles section, located in the Asturias community in Northern Spain (Fig. 1). Presented data from the Spanish section reveals the presence of several relevant climate changes which have been correlated with the results obtained in different sections of Europe, showing that these climatic changes, as well as the documented perturbations of the carbon cycle, could be of global, or at least of regional extent at the European scale.

2 Materials and methods

The 110 m thick studied section composed of 562 beds has been studied bed by bed. Collected ammonites were prepared and studied following the usual palaeontological methods. The obtained biochronostratigraphy allowed characterization of the standard chronozones and subchronozones established by Elmi et al. (1997) and Page (2003), which are used in this work.

A total of 191 analyses of stable isotopes were performed on 163 belemnite calcite samples, in order to obtain the primary Late Sinemurian, Pliensbachian and Early Toarcian seawater stable isotope signal, and hence to determine palaeotemperature changes, as well as the variation pattern of the carbon isotope in the studied time interval. For the assessment of possible burial diagenetic alteration of the belemnites, polished samples and thick sections of each belemnite rostrum were prepared. The thick sections were studied under the petrographic and the cathodoluminescence microscope, and only the non-luminescent, diagenetically unaltered portions of the belemnite rostrum, were sampled using a microscope-mounted dental drill. Belemnites in the Rodiles section generally show an excellent degree of preservation (Fig. 2) and none of the prepared samples were rejected, as only the parts of the belemnite rostrum not affected by diagenesis were selected. Sampling of the luminescent parts such as the apical line and the outer and inner rostrum wall, fractures, stylolites and borings were avoided. Belemnite calcite was processed in the stable isotope labs of the Michigan University (USA), using a Finnigan MAT 253 triple collector isotope ratio mass spectrometer. The procedure followed in the stable isotope analysis has been described in Gómez and Goy (2011). Isotope ratios are reported in per mil relative to the standard Peedee belemnite (PDB), having a reproducibility better than 0.02 ‰ PDB for $\delta^{13}C$ and better than 0.06 ‰ PDB for $\delta^{18}O$.

The seawater palaeotemperature recorded in the oxygen isotopes of the studied belemnite rostra have been calculated using the Anderson and Arthur (1983) equation: $T(ºC) = 16.0 - 4.14\ (\delta_c - \delta_w) + 0.13\ (\delta_c - \delta_w)^2$ where $\delta_c = \delta^{18}O$ PDB is the composition of the sample, and $\delta_w = \delta^{18}O$ SMOW the composition of ambient seawater. According to the recommendations of Shackleton and Kennett (1975), the standard value of $\delta_w = -1$‰ was used for palaeotemperature calculations under non-glacial ocean water conditions. If the presence of permanent ice caps in the poles is demonstrated for some of the studied intervals, value of $\delta_w = 0$‰ would be used and consequently calculated palaeotemperatures would increase in the order of 4ºC.

Discussion on the palaeoecology of belemnites and the validity of the isotopic data obtained from belemnite calcite for the calculation of palaeotemperatures is beyond the scope of this paper. The use of belemnite calcite as a proxy is generally accepted and widely used as a reliable tool for palaeothermometry in most of the Mesozoic. However, palaeoecology of belemnites is a source of discrepancies because, as extinct organisms, there is a complete lack of understanding of fossil belemnite ecology (Rexfort and Mutterlose, 2009). Belemnite lived as active predators with a swimming mode of life. Nevertheless, several authors (Anderson et al., 1994; Mitchell, 2005; Wierzbowski and Joachimiski, 2007) proposed a bottom-dwelling mode of life on the basis of oxygen isotope thermometry, similar to modern sepiids which show a necktobenthic mode of life. This is contradicted by the occurrence of various belemnite genera in black shales that lack any benthic or necktobenthic organisms due

to anoxic bottom waters (i.e. the Lower Jurassic Posidonienschiefer, see Rexfort and Mutterlose, 2009), indicating that belemnites had a necktonic rather than a necktobenthic mode of life (Mutterlose et al., 2010). As Rexfort and Mutterlose (2009) stated, It is unclear whether isotopic data from belemnites reflect a surface or a deeper water signal and we do not know if the belemnites mode of life changed during ontogeny. Similarly, Li et al., (2012) concluded that belemnites were mobile and experienced a range of environmental conditions during growth. Some belemnite species inhabited environmental niches that remain unchanged, while other species had a more cosmopolitan lifestyle inhabiting wider environments. To complete the scenario, Mutterlose et al. (2010) suggested different lifestyles (nektonic versus necktobenthic) of belemnites genera as indicated by different shaped guards. Short, thick guards could indicate necktobentic lifestyle, elongated forms fast swimmers, and extremely flattened guards benthic lifestyle.

The Ullmann et al. (2014) work hypothesises that belemnites (*Passaloteuthis*) of the Lower Toarcian Tenuicostatum Zone had a necktobenthic lifestyle and once became extinct (as many organisms in the Early Toarcian mass extinction) were substituted by belemnites of the genus *Acrocoelites* supposedly of nektonic lifestyle that these authors impute as due to anoxia.

On the other hand, the isotopic studies performed on present-day cuttlefish (*Sepia* sp.), which are assumed to be the most similar group equivalent to belemnites, reveals that all the analyzed specimens (through their $\delta^{18}O$ signal) reflect the temperature-characteristics of their habitat perfectly (Rexfort and Mutterlose, 2009). Also the studies of Bettencourt and Guerra (1999), performed in cuttlebone of *Sepia officinalis* conclude that the obtained $\delta^{18}O$ temperature agreed with changes in temperature of seawater, supporting the use of belemnites as excellent tools for calculation of palaeotemperatures.

It seems that at least some belemnites could swim through the water column, reflecting the average temperature and not necessarily only the temperature of the bottom water or of the surface water. In any case, instead of single specific values, comparisons of average temperatures to define the different episodes of temperature changes are used in this work.

For palaeotemperature calculation, it has been assumed that the $\delta^{18}O$ values, and consequently the resultant curve, essentially reflects changes in environmental parameters (Sælen et al., 1996; Bettencourt and Guerra, 1999; McArthur et al., 2007; Price et al., 2009; Rexfort and Mutterlose, 2009; Benito and Reolid, 2012; Li et al., 2012; Harazim et al., 2013; Ullmann et al., 2014, Ullmann and Korte, 2015), as the sampled non-luminescent biogenic calcite of the studied belemnite rostra precipitated in equilibrium with the seawater. It has also being assumed that the biogenic calcite retains the primary isotopic composition of the seawater and that the belemnite migration, skeletal growth, the sampling bias, and the vital effects are not the main factors responsible for the obtained variations. Cross-plot of the $\delta^{18}O$ against the $\delta^{13}C$ values (Fig. 3) reveals a cluster type of distribution, showing a negative correlation coefficient (–0.2) and very low covariance (R^2=0.04), supporting the lack of digenetic overprints in the analyzed diagenetically screened belemnite calcite.

3 Results

In the coastal cliffs located northeast of the Villaviciosa village, in the eastern part of the Asturias community (Northern Spain) (Fig. 1), the well exposed Upper Sinemurian, Pliensbachian and Lower Toarcian deposits are represented by a succession of alternating lime mudstone to bioclastic wackestone and marls with interbedded black shales belonging to the Santa Mera Member of the Rodiles Formation (Valenzuela, 1988) (Fig. 4). The uppermost Sinemurian and Pliensbachian deposits have been studied in the eastern part of the Rodiles Cape and the uppermost Pliensbachian and Lower Toarcian in the western part of the Rodiles Cape (West Rodiles section of Gómez et al., 2008; Gómez and Goy 2011). Both fragments of the section are referred here as the Rodiles section (lat. 43º32'22" long.5º22'22"). Palaeogeographical reconstruction based on comprehensive palaeomagnetic data, carried out by Osete et al. (2010), locates the studied Rodiles section at a latitude of about 32º N for the Hettangian–Sinemurian interval and at a latitude of almost 40º N (the current latitude of Madrid) for the Toarcian–Aalenian interval.

Ammonite taxa distribution and profiles of the $\delta^{18}O_{bel}$, $\delta^{13}C_{bel}$ and $\delta^{13}C_{bulk}$ values obtained from belemnite calcite have been plotted against the 562 measured beds of the Rodiles section (Fig. 5).

3.1 Lithology

The Upper Sinemurian, Pliensbachian and Lower Toarcian deposits of the Rodiles section are constituted by couplets of bioclastic lime mudstone to wackestone limestone and marls. Occasionally the limestones contain bioclastic packstone facies concentrated in rills. Limestones, generally recrystallized to microsparite, are commonly well stratified in beds whose continuity can be followed at the outcrop scale, as well as in outcrops several kilometres apart. However, nodular limestone layers, discontinuous at the outcrop scale, are also present. The base of some carbonates can be slightly erosive, and they are commonly bioturbated, to reach the homogenization stage. Ichnofossils, specially *Thalassinoides, Chondrites* and *Phymatoderma,* are also present. Marls, with $CaCO_3$ content generally lower than 20% (Bádenas et al., 2009, 2012), are frequently gray coloured, occasionally light gray due to the higher proportion of carbonates, with interbedded black intervals. Locally brown coloured sediments, more often in the Upper Sinemurian, are present.

3.2 Biochronostratigraphy

The ammonite-based biochronostratigraphy of these deposits in Asturias have been carried out by Suárez-Vega (1974), and the uppermost Pliensbachian and Toarcian ammonites by Gómez et al. (2008), and by Goy et al. (2010 a, b). Preliminary biochronostratigraphy of the Late Sinemurian and the Pliensbachian in some sections of the Asturian Basin has been reported by Comas-Rengifo and Goy (2010), and the result of more than ten years of bed by bed sampling of ammonites in the Rodiles section, which allowed precise time constrain for the climatic events described in this work, are here summarized.

Collected ammonites allowed the recognition of all the standard Late Sinemurian, Pliensbachian and Early Toarcian chronozones and subchronozones defined by Elmi et

al. (1997) and Page (2003) for Europe. Section is generally expanded and ammonites are common enough as to constrain the boundaries of the biochronostratigraphical units. Exceptions are the Taylori−Polymorphus subchronozones that could not be separated, and the Capricornus−Figulinum subchronozones of the Davoei Chronozone, partly due to the relatively condensed character of this Chronozone. Most of the recorded species belong to the NW Europe province but some representatives of the Tethysian Realm are also present.

3.3 Carbon isotopes

The carbon isotopes curve reflects several oscillations through the studied section (Fig. 5). A positive $\delta^{13}C_{bel}$ shift, showing average values of 1.6‰ is recorded in the Late Sinemurian Densinodulum to part of the Macdonnelli subchronozones. From the latest Sinemurian Aplanatum Subchronozone (Raricostatum Chronozone) up to the Early Pliensbachian Valdani Subchronozone of the Ibex Chronozone, average $\delta^{13}C_{bel}$ values are −0.1‰, delineating an about 1−1.5‰ relatively well marked negative excursion. In the late Ibex and in the Davoei chronozones, the $\delta^{13}C_{bel}$ curve records background values of about 1‰, with a positive peak at the latest Ibex Chronozone and the earliest Davoei Chronozone.

At the Late Pliensbachian the $\delta^{13}C_{bel}$ values tend to outline a slightly positive excursion, interrupted by a small negative peak in the latest Spinatum Chronozone. The Early Toarcian curve reflects the presence of a positive $\delta^{13}C_{bel}$ trend which develops above the here represented stratigraphical levels, up to the Middle Toarcian Bifrons Chronozone (Gómez et al., 2008) and a negative excursion recorded in bulk carbonates samples.

3.4 Oxygen isotopes

The $\delta^{18}O_{bel}$ values show the presence of several excursions through the Late Sinemurian to the Early Toarcian (Fig. 5). In the Late Sinemurian to the earliest Pliensbachian interval, an about 1‰ negative excursion, showing values generally below −1‰ with peak values up to −3‰ has been recorded in Sinemurian samples located immediately below the stratigraphic column represented in Fig. 5. In most of the Early Pliensbachian Jamesoni and the earliest part of the Ibex chronozones, $\delta^{18}O_{bel}$ values are quite stable, around −1‰, but another about 1−1.5‰ negative excursion, with peak values up to −1.9‰, develops along most of the Early Pliensbachian Ibex and Davoei chronozones, extending up to the base of the Late Pliensbachian Margaritatus Chronozone. Most of the Late Pliensbachian and the earliest Toarcian are characterized by the presence of an important change. A well-marked in the order of 1.5‰ $\delta^{18}O_{bel}$ positive excursion, with frequent values around 0‰, and positive values up to 0.7‰, were assayed in this interval. The oxygen isotopes recorded a new change on its tendency in the Early Toarcian, where a prominent $\delta^{18}O_{bel}$ negative excursion, about 1.5–2‰ with values up to −3‰, has been verified.

4 Discussion

The isotope curves obtained in the Upper Sinemurian, Pliensbachian and Lower Toarcian section of the Asturian Basin has been correlated with other successions of similar age, in order to evaluate if the recorded environmental features have a local or

a possible global extent. In order to correlate a more homogeneous dataset, only the isotopic results obtained by other authors from belemnite calcite and exceptionally from brachiopod calcite, have been used for the correlation of the stable isotopic data.

4.1 Carbon isotope curve

The $\delta^{13}C_{bel}$ carbon isotope excursions (CIEs) found in the Asturian Basin, can be followed in other sections across Western Europe (Fig. 6). The Late Sinemurian positive CIE has also been recorded in the Cleveland Basin of the UK by Korte and Hesselbo (2011) and in the $\delta^{13}C_{org}$ data of the Wessex Basin of southern UK by Jenkyns and Weedon (2013).

The Early Pliensbachian $\delta^{13}C_{bel}$ negative excursion that extends from the Raricostatum Chronozone of the latest Sinemurian to the Early Pliensbachian Jamesoni and part of the Ibex chronozones (Fig. 6), correlates with the lower part of the $\delta^{13}C_{bel}$ negative excursion reported by Armendáriz et al. (2012) in another section of the Asturian Basin. Similarly, the $\delta^{13}C_{bel}$ curve obtained by Quesada et al. (2005) in the neighbouring Basque–Cantabrian Basin, shows the presence of a negative CIE in similar stratigraphical position. In the Cleveland Basin of the UK, the studies on the Sinemurian–Pliensbachian deposits carried out by Hesselbo et al. (2000), Jenkyns et al. (2002) and Korte and Hesselbo (2011) reflect the presence of this Early Pliensbachian $\delta^{13}C_{bel}$ negative excursion. In the Peniche section of the Lusitanian Basin of Portugal, this negative CIE has also been recorded by Suan et al. (2010) in brachiopod calcite, and in bulk carbonates in Italy (Woodfine et al., 2008; Francheschi et al., 2014). The about 1.5–2‰ magnitude of this negative excursion seems to be quite consistent across the different European localities.

Korte and Hesselbo (2011) pointed out that the Early Pliensbachian $\delta^{13}C$ negative excursion seems to be global in character and the result of the injection of isotopically light carbon from some remote source, such as methane from clathrates, wetlands, or thermal decomposition or thermal metamorphism or decomposition of older organic-rich deposits. However none of these possibilities have been documented yet.

Higher in the section, the $\delta^{13}C$ values are relatively uniform, except for a thin interval, around the Early Pliensbachian Ibex–Davoei zonal boundary, where a small positive peak (the Ibex–Davoei positive peak, previously mentioned by Rosales et al., 2001 and by Jenkyns et al., 2002) can be observed in most of the $\delta^{13}C$ curves summarized in Fig. 6, as well as in the carbonates of the Portuguese Lusitanian Basin (Silva et al., 2011).

The next CIE is a positive excursion about 1.5–2‰, well recorded in all the correlated Upper Pliensbachian sections (the Late Pliensbachian positive excursion in Fig. 6) and in bulk carbonates of the Lusitanian Basin (Silva et al., 2011). Around the Pliensbachian–Toarcian boundary, a negative $\delta^{13}C$ peak is again recorded (Fig. 6). This narrow excursion was described by Hesselbo et al. (2007) in bulk rock samples in Portugal, and tested by Suan et al. (2010) in the same basin and extended to the Yorkshire (UK) by Littler et al. (2010) and by Korte and Hesselbo (2011). If this perturbation of the carbon cycle is global, as Korte and Hesselbo (2011) pointed out, it could correspond with the negative $\delta^{13}C$ peak recorded in the upper part of the Spinatum Chronozone in the Asturian Basin (this work); with the negative $\delta^{13}C$ peak

reported by Quesada et al. (2005) in the same stratigraphical position in the Basque–Cantabrian Basin, and with the $\delta^{13}C$ negative peak reported by van de Schootbrugge et al. (2010) and Harazim et al. (2013) in the French Grand Causses Basin.

Finally, the Early Toarcian is characterized by a prominent $\delta^{13}C$ positive excursion that has been detected in all the here considered sections, as well as in some South American (Al-Suwaidi et al., 2010) and Northern African (Bodin et al., 2010) sections, which is interrupted by an about 1‰ $\delta^{13}C_{bulk}$ negative excursion located around the Tenuicostatum–Serpentinum zonal boundary.

The origin of the positive excursion has been interpreted by some authors as the response of water masses to excess and rapid burial of large amounts of organic carbon rich in ^{12}C, which led to enrichment in ^{13}C of the sediments (Jenkyns and Clayton, 1997; Schouten et al., 2000). Other authors ascribe the origin of this positive excursion to the removal from the oceans of large amounts of isotopically light carbon as organic matter into black shales or methane hydrates, resulting from ebullition of isotopically heavy CO_2, generated by methanogenesis of organic-rich sediments (McArthur et al., 2000).

Although $\delta^{13}C$ positive excursions are difficult to account for (Payne and Kump, 2007), it seems that this $\delta^{13}C$ positive shift cannot necessarily be the consequence of the widespread preservation of organic-rich facies under anoxic waters, as no anoxic facies are present in the Spanish Lower Toarcian sections (Gómez and Goy, 2011). Modelling of the CIEs performed by Kump and Arthur (1999) shows that $\delta^{13}C$ positive excursions can also be due to an increase in the rate of phosphate or phosphate and inorganic carbon delivery to the ocean, and that large positive excursions in the isotopic composition of the ocean can also be due to an increase in the proportion of carbonate weathering relative to organic carbon and silicate weathering. Other authors argue that increase of $\delta^{13}C$ in bulk organic carbon may reflect a massive expansion of marine archaea bacteria that do not isotopically discriminate in the type of carbon they use, leading to positive $\delta^{13}C$ shifts (Kidder and Worsley, 2010).

The origin of the Early Toarcian $\delta^{13}C$ negative excursion has been explained by several papers as due to the massive release of large amounts of isotopically light CH_4 from the thermal dissociation of gas hydrates Hesselbo et al. (2000, 2007), Cohen et al. (2004) and Kemp et al. (2005), with the massive release of gas methane linked with the intrusion of the Karoo-Ferrar large igneous province onto coalfields, as proposed by McElwain et al. (2005) or with the contact metamorphism by dykes and sills related to the Karoo-Ferrar igneous activity into organic-rich sediments (Svensen et al., 2007).

4.2. Oxygen isotope curves and seawater palaeotemperature oscillations

Seawater palaeotemperature calculation from the obtained $\delta^{18}O$ values reveals the occurrence of several isotopic events corresponding with relevant climatic oscillations across the latest Sinemurian, the Pliensbachian and the Early Toarcian (Fig. 7). Some of these climatic changes could be of global extent. In terms of seawater palaeotemperature, five intervals can be distinguished. The earliest interval corresponds with a warming period developed during the Late Sinemurian up to the

earliest Pliensbachian. Most of the Early Pliensbachian is represented by a period of "normal" temperature, close to the average palaeotemperatures of the studied interval. A new warming period is recorded at the Early–Late Pliensbachian transition, and the Late Pliensbachian is represented by an important cooling interval. Finally the Early Toarcian coincides with a severe (super)warming interval, linked to the important Early Toarcian mass extinction (Gómez and Arias, 2010; García Joral et al., 2011; Gómez and Goy, 2011; Fraguas et al., 2012; Clémence, 2014; Clémence et al., 2015; Baeza-Carratalá et al., 2015).

The average palaeotemperature of the latest Sinemurian, Pliensbachian (palaeolatitude of 32ºN) and Early Toarcian (palaeolatitude of 40ºN), calculated from the $\delta^{18}O$ values obtained from belemnite calcite in this work, is 15.6ºC.

4.2.1 The Late Sinemurian Warming

The earliest isotopic event is a $\delta^{18}O$ negative excursion that develops in the Late Sinemurian Raricostatum Chronozone, up to the earliest Pliensbachian Jamesoni Chronozone. Average palaeotemperatures calculated from the $\delta^{18}O$ belemnite samples collected below the part of the Late Sinemurian Raricostatum Chronozone represented in figure 5 were 19.6ºC. This temperature increases to 21.5ºC in the lower part of the Raricostatum Chronozone (Densinodulum Subchronozone), and temperature progressively decreases through the latest Sinemurian and earliest Pliensbachian. In the Raricostaum Subchronozone, the average calculated temperature is 18.7ºC; in the Macdonnelli Subchronozone average temperature is 17.5ºC and average values of 16.7ºC, closer to the average temperatures of the studied interval, are not reached until the latest Sinemurian Aplanatum Subchronozone and the earliest Pliensbachian Taylori–Polymorphus subchronozones. All these values delineate a warming interval mainly developed in the Late Sinemurian (Figs. 7, 8).

The Late Sinemurian Warming interval is also recorded in the Cleveland Basin of the UK (Hesselbo et al., 2000; Korte and Hesselbo, 2011). The belemnite-based $\delta^{18}O$ values obtained by these authors are in the order of –1‰ to –3‰, with peak values lower than –4‰. That represents a range of palaeotemperatures normally between 16 and 24ºC with peak values up to 29ºC, which are not compatible with a cooling, but with a warming interval.

The Late Sinemurian warming coincides only partly with the Early Pliensbachian $\delta^{13}C$ negative excursion, located near the stage boundary (Fig. 6). Consequently, this warming cannot be fully interpreted as the consequence of the release of methane from clathrates, wetlands or decomposition of older organic-rich sediments, as interpreted by Korte and Hesselbo (2011) because only a small portion of both excursions are coincident.

4.2.2 The "normal" temperature Early Pliensbachian Jamesoni Chronozone interval

After the Late Sinemurian Warming, $\delta^{18}O$ values are around –1‰ reflecting average palaeotemperatures of about 16ºC (Fig. 7). This Early Pliensbachian interval of "normal" (average) temperature develops in most of the Jamesoni Chronozone and the base of the Ibex Chronozone (Fig. 8). In the Taylori–Polymorphus chronozones, average temperature is 15.7ºC, in the Brevispina Subchronozone is 16.4ºC, and in the

Jamesoni Subchronozone 17.2ºC. Despite showing more variable data, this interval has also been recorded in other sections of the Asturian Basin (Fig. 8) by Armendáriz et al. (2012), and relatively uniform values are also recorded in the Basque–Cantabrian Basin of Northern Spain (Rosales et al., 2004) and in the Peniche section of the Portuguese Lusitanian Basin (Suan et al., 2008, 2010). Belemnite calcite-based $\delta^{18}O$ values published by Korte and Hesselbo (2011) are quite scattered, oscillating between ~1‰ and ~–4.5‰ (Fig. 8).

4.2.3 The Early Pliensbachian Warming interval

Most of the Early Pliensbachian Ibex Chronozone and the base of the Late Pliensbachian are dominated by a 1 to 1.5‰ $\delta^{18}O$ negative excursion, representing an increase in palaeotemperature, which marks a new warming interval. Average values of 18.2 ºC with peak values of 19.7ºC were reached in the Rodiles section (Fig. 7). This increase in temperature partly co-occurs with the latest part of the Early Pliensbachian $\delta^{13}C$ negative excursion.

The Early Pliensbachian Warming interval is also well marked in other sections of Northern Spain (Fig. 8) like in the Asturian Basin (Armendáriz et al., 2012) and the Basque–Cantabrian Basin (Rosales et al., 2004), where peak values around 25ºC were reached. The increase in seawater temperature is also registered in the Southern France Grand Causses Basin (van de Schootbrugge et al., 2010), where temperatures averaging around 18ºC have been calculated. This warming interval is not so clearly marked in the brachiopod calcite of the Peniche section in Portugal (Suan et al., 2008, 2010), but even very scattered $\delta^{18}O$ values, peak palaeotemperature near 30ºC were frequently reported in the Cleveland Basin (Korte and Hesselbo, 2011). In the compilation performed by Dera et al. (2009, 2011), $\delta^{18}O$ values are quite scattered, but this Early Pliensbachian Warming interval is also well marked, supporting a possible global extent for this climatic event.

4.2.4 The Late Pliensbachian Cooling interval

One of the most important Jurassic $\delta^{18}O$ positive excursions is recorded at the Late Pliensbachian and the earliest Toarcian in all the correlated localities (Figs. 5, 7, 8). This represents an important climate change towards cooler temperatures that begins at the base of the Late Pliensbachian and extends up to the earliest Toarcian Tenuicostatum Chronozone, representing an about 4 Myrs major cooling interval. Average palaeotemperatures of 12.7ºC for this period in the Rodiles section have been calculated, and peak temperatures as low as 9.5ºC were recorded in several samples from the Gibbosus and the Apyrenum subchronozones (Fig. 7).

This major cooling event has been recorded in many parts of the World. In Europe, the onset and the end of the cooling interval seems to be synchronous at the scale of ammonites subchronozone (Fig. 8). It starts at the Stokesi Subchronozone of the Margaritatus Chronozone (near the onset of the Late Pliensbachian), and extends up to the Early Toarcian Semicelatum Subchronozone of the Tenuicostatum Chronozone. In addition to the Asturian Basin (Gómez et al., 2008; Gómez and Goy, 2011; this work), it has clearly been recorded in the Basque–Cantabrian Basin (Rosales et al., 2004; Gómez and Goy, 2011; García Joral et al., 2011) and in the Iberian Basin of Central Spain

(Gómez et al., 2008; Gómez and Arias, 2010; Gómez and Goy, 2011), in the Cleveland Basin of the UK (McArthur et al., 2000; Korte and Hesselbo, 2011), in the Lusitanian Basin (Suan et al., 2008, 2010), in the French Grand Causses Basin (van de Schootbrugge et al., 2010), and in the data compiled by Dera et al. (2009, 2011).

As for many of the major cooling periods recorded in the Phanerozoic, low levels of atmospheric pCO_2, and/or variations in oceanic currents related to the break-up of Pangea could explain these changes in seawater (Dera et al., 2009; 2011). The presence of relatively low pCO_2 levels in the Late Pliensbachian atmosphere is supported by the value of ~900 ppm obtained from Pliensbachian araucariacean leaf fossils of southeastern Australia (Steinthorsdottir and Vajda, 2015). These values are much higher than the measured Quaternary preindustrial 280 ppm CO_2 (i.e. Wigley et al., 1996), but lower than the ~1000 ppm average estimated for the Early Jurassic. The recorded Pliensbachian values represent the minimum values of the Jurassic and of most of the Mesozoic, as documented by the GEOCARB II (Berner, 1994), and the GEOCARB III (Berner and Kothavala, 2001) curves, confirmed for the Early Jurassic by Steinthorsdottir and Vajda (2015). Causes of this lowering of atmospheric pCO_2 are unknown but they could be favoured by elevated silicate weathering rates, nutrient influx, high primary productivity, and organic matter burial (Dromart et al., 2003).

It seems that the Late Pliensbachian represents a time interval of major cooling, probably of global extent. This fact has conditioned that many authors point to this period as one of the main candidates for the development of polar ice caps in the Mesozoic (Price, 1999; Guex et al., 2001; Dera et al., 2011; Suan et al., 2011; Gómez and Goy, 2011; Fraguas et al., 2012). This idea is based on the presence, in the Upper Pliensbachian deposits of different parts of the World, of: 1) glendonites; 2) exotic pebble to boulder-size clasts; 3) the presence in some localities of a hiatus in the Late Pliensbachian–earliest Toarcian; 4) the results obtained in the General Circulation Models, and 5) the calculated Late Pliensbachian palaeotemperatures and the assumed pole-to-equator temperature gradient.

4.2.5 The presence of glendonites of Pliensbachian age

It is assumed that glendonite, a calcite pseudomorph after the metastable mineral ikaite, grows in marine deposits under near-freezing temperatures (0–4ºC), at or just below the sediment–water interface. This mineral is commonly associated with organic-rich sediments, where methane oxidation is occurring, and is favoured by high alkalinity and elevated concentrations of dissolved orthophosphate (e.g. De Lurio and Frakes, 1999; Selleck et al., 2007). Based on these features, glendonites have been extensively used as a robust indicator of cold water palaeotemperature in organic-rich environments during the periods of ikaite growth. Oxygen isotope data of modern ikaite suggests that carbonate precipitation is in equilibrium with ambient seawater, but carbon isotope signatures are normally very negative, up to –33.9‰ in the Recent deep marine deposits of the Zaire Fan (Jansen et al., 1987) consistent with derivation of carbonate from methane oxidation.

The presence of glendonite in deposits of Pliensbachian age has been reported from Northern Siberia (Kaplan, 1978; Rogov and Zakharov, 2010; Devyatov, et al., 2010; Suan et al., 2011), and the occurrence of this pseudomorph in Pliensbachian deposits

of circum polar palaeolatitudes has been considered as a strong support for the interpretation of near-freezing to glacial climate conditions (Price, 1999; Suan et al., 2011). However, Teichert and Luppold (2013) reported the presence of three horizons with glendonites in Upper Pliensbachian (Margaritatus to Spinatum zones) methane seeps in Germany, where belemnite and ostracod-based calculated bottom water palaeotemperature were ca. 10ºC, which was well above the previously observed near freezing range of ikaite stability. As a consequence, these authors raised the question if methane seeps are geochemical sites where ikaite can be formed at higher temperatures due to methanotrophic sulphate reduction as the triggering geochemical process for ikaite formation at the sulphate-methane interface. The possibility of ikaite formation at higher than previously expected temperatures needs experimental confirmation, but until these data are available, the use of glendonite as unequivocal indicator of near-freezing palaeotemperature should be cautioned.

4.2.6 Exotic clasts rafted by ice

Exotic pebble to boulder-size clasts of Pliensbachian age, have been described in Northern Siberia by several papers (Kaplan, 1978; Rogov and Zakharov, 2010; Devyatov et al., 2010; Suan et al., 2011). They are composed of limestone, marly limestone and basalt clasts, included in a succession of interbedded sandstone, siltstone and silty clay. These deposits have been interpreted as ice-rafted dropstones and have been taken as an evidence of near-freezing climatic conditions in the Artic region (Price, 1999; Suan et al., 2011).

4.2.7 Short-lived regression forced by cooling and glaciations

The presence of a hiatus around the Pliensbachian–Toarcian boundary in some (but not all) European, North African, South American and Siberian sections (Guex, 1973; Guex et al., 2001, 2012; Suan et al., 2011) has been interpreted as the result of a major short-lived regression, forced by cooling that reached near freezing to glacial conditions, derived from increased volcanic activity (Guex et al., 2001, 2012).

From the here presented data, the interval of cooling development can now be precisely constrained. Low seawater temperatures started at the Late Pliensbachian Stokesi Subchronozone of the Margaritatus Chronozone and ended at the earliest Toarcian Semicelatum Subchronozone of the Tenuicostatum Chronozone, spanning virtually along all the Late Pliensbachian and the base of the Early Toarcian. In terms of time, the duration of the cooling interval spans for about 4 Myr (Ogg, 2004; Ogg and Hinnov, 2012). Even it cannot be fully discarded, it seems quite inconsistent to attribute the end-Pliensbachian–earliest Toarcian regression to the presence of glacial conditions right at the end of the cold climatic interval. If cooling was able to produce enough ice volume in the pole caps as to generate a generalized lowstand period, important enough as to provoke a generalized hiatus, the amplitude of this hiatus would virtually affect the whole Late Pliensbachian, whilst in reality only affects in some places, not in all areas, to a few ammonite chronozones, and mainly of the earliest Toarcian.

On the other hand, no major volcanic activity responsible for the climatic change was recorded at the Late Pliensbachian. The Karoo-Ferrar volcanism did not start until the

Early Toarcian (Svensen et al., 2007; Jourdan et al., 2007, 2008; Moulin et al., 2011; Dera et al., 2011; Ogg and Hinnov, 2012; Sell et al., 2014; Burgess et al., 2015; Percival et al., 2015), and only minor Pliensbachian volcanism has been reported in the North Sea and in the Patagonia (Dera et al., 2011) as well as in the Iberian Range of Central Spain (Cortés, 2015). The recorded volcanism does not seem to be important enough as to release the huge amount of SO_2 needed to change the climate of the Earth, as Guex et al. (2012) proposed.

4.2.8 Late Pliensbachian palaeotemperatures and the pole-to-equator temperature gradient.

The idea of a Jurassic latitudinal climate gradient in Eurasia significantly lower than today, with winter temperatures in Siberia probably never falling below 0ºC (Frakes et al., 1992) as well as warmer, more equable conditions compared to the present day, with no ice caps in the polar region (Hallam, 1975) has been the dominant opinion for many years.

This assumption is mainly based on the supposed wide distribution of part of the Jurassic flora, like the absence of the vascular plants of the genus *Xenoxylon* at high latitudes (Philippe and Thevenard, 1996), and the distribution of fauna and of sedimentary facies (Hallam, 1975). This opinion was maintained against the incipient studies of $\delta^{18}O$-based palaeotemperature that already indicated the presence of significant climate changes during the Jurassic (Stevens and Clayton, 1971).

The presence of a marked pole-to-equator climate and particularly temperature gradient during the Jurassic times has been evidenced by several studies. As an example, the manifest bipolarity in the distribution of certain bivalves has been documented by Crame (1993), particularly for the Pliensbachian and the Tithonian. Also Hallam (1972) denoted an increasing diversity gradient in the Pliensbachian and Toarcian from the Tethyan to the Boreal domains and Liu et al. (1998) reported that temperature gradients were one of the main factors for Jurassic bivalve's provincialism. More recently, Damborenea et al., (2013) documented the latitudinal gradient and bipolar distribution patterns at a regional and global scale shown by marine bivalves during the Triassic and the Jurassic.

Provinciality among Ammonoids has been classically recognized (i.e. Dommergues et al., 1997; Enay and Cariou, 1997; Cecca, 1999; Page, 2003, 2008; Dera et al., 2010), including seawater temperature as one of the major factors controlling their latitudinal distribution. Jurassic brachiopods show also good examples of latitudinal distribution, where temperature has been considered one of the most important factors (i.e. García Joral et al., 2011).

The presence of pole-to-equator temperature gradient, shown by several fossil groups, lends support to the presence of cold or even freezing conditions at the poles (Price, 1999). In addition, the Chandler et al. (1992) general circulation model (GCM) simulation for the Early Jurassic, concluded that winter temperatures within the continental interiors dropped to about −32ºC, and seasonal range over high latitude mountains surpass 45ºC, similar to the current seasonality of Siberia. These conditions are compatible with the formation of permanent or seasonal ice in the Polar Regions.

4.2.9 The Early Toarcian Warming interval

Seawater temperature started to increase at the earliest Toarcian. From an average temperature of 12.7ºC during the Late Pliensbachian Cooling interval, average temperature rose to 15ºC in the upper part of the earliest Toarcian Tenuicostatum Chronozone (Semicelatum Subchronozone), which represents a progressive increase on seawater temperature in the order of 2–3ºC. Atmospheric CO_2 concentration during the Early Toarcian seems to be doubled from ~1000 ppm to ~2000 ppm (i.e. Berner, 2006; Retallack, 2009; Steinthorsdottir and Vajda, 2015), causing this important and rapid warming.

Comparison of the evolution of palaeotemperature with the evolution of the number of taxa reveals that progressive warming coincides first with a progressive loss in the taxa of several groups (Gómez and Arias, 2010; Gómez and Goy, 2011; García Joral et al., 2011; Fraguas et al., 2012; Baeza-Carratalá et al., 2015) marking the prominent Early Toarcian extinction interval. Seawater palaeotemperature rapidly increased around the Tenuicostatum–Serpentinum zonal boundary, where average values of about 21ºC, with peak temperatures of 24ºC were reached (Fig. 7). This important warming, which represents a ΔT of about 8ºC respect to the average temperatures of the Late Pliensbachian Cooling interval, coincides with the turnover of numerous groups (Gómez and Goy, 2011) the total disappearance of the brachiopods (García Joral et al., 2011; Baeza-Carratalá et al., 2015), the extinction of numerous species of ostracods (Gómez and Arias, 2010), and a crisis of the nannoplankton (Fraguas, 2010; Fraguas et al., 2012; Clémence et al., 2015). Temperatures remain high and relatively constant through the Serpentinum and Bifrons chronozones, and the platforms were repopulated by opportunistic immigrant species that thrived in the warmer Mediterranean waters (Gómez and Goy, 2011).

5. Conclusions

Several relevant climatic oscillations across the Late Sinemurian, the Pliensbachian and the Early Toarcian have been documented in the Asturian Basin. Correlation of these climatic changes with other European records points out that some of them could be of global extent. In the Late Sinemurian, a warm interval showing average temperature of 18.5ºC was recorded. The end of this warming interval coincides with the onset of a $\delta^{13}C$ negative excursion that develops through the latest Sinemurian and part of the Early Pliensbachian.

The Late Sinemurian Warming interval is followed by an interval of “normal” temperature averaging 16ºC, which develops through most of the Early Pliensbachian Jamesoni Chronozone and the base of the Ibex Chronozone.

The latest part of the Early Pliensbachian is dominated by an increase in temperature, marking another warming interval which extends to the base of the Late Pliensbachian, where average temperature of 18.2 ºC was calculated. Within this warming interval, a $\delta^{13}C$ positive peak occurs at the transition between the Early Pliensbachian Ibex and Davoei chronozones.

One of the most important climatic changes was recorded through the Late Pliensbachian. Average palaeotemperature of 12.7ºC for this interval in the Rodiles

section delineated an about 4 Myrs major Late Pliensbachian Cooling event that was recorded in many parts of the World. At least in Europe, the onset and the end of this cooling interval is synchronous at the scale of ammonites subchronozone. The cooling interval coincides with a $\delta^{13}C$ slightly positive excursion, interrupted by a small negative $\delta^{13}C$ peak in the latest Pliensbachian Hawskerense Chronozone.

This prominent cooling event has been pointed as one of the main candidates for the development of polar ice caps in the Jurassic. Even some of the exposed data need additional studies, like the meaning of the glendonite, and that more updated GMC studies are required; most of the available data support the hypothesis that ice caps were developed during the Late Pliensbachian Cooling interval.

Seawater temperature started to increase at the earliest Toarcian, rising to 15ºC in the latest Tenuicostatum Chronozone (Semicelatum Subchronozone), and seawater palaeotemperature considerably increased around the Tenuicostatum−Serpentinum zonal boundary, reaching average values in the order of 21ºC, with peak intervals of 24ºC, which coincides with the Early Toarcian major extinction, pointing warming as the main cause of the faunal turnover.

Acknowledgments

Prof. Appy Sluijs and two anonymous reviewers are thanked for their comments and suggestions that improved the manuscript. This research work was financed by projects CGL 2011−25894 and CGL2011-23947 (MICINN) of the Spanish Ministerio de Economía y Competitividad, and by projects GR3/14/910431, and GI 910429 of the Universidad Complutense de Madrid. Thanks to the Instituto Geológico y Minero de España for allowing the use of the cathodoluminescence microscope.

References

Al-Suwaidi, A.H., Angelozzi, G.N., Baudin, F., Damborenea, S.E., Hesselbo, S.P., Jenkyns, H.C., Manceñido, M.O. and Riccardi, A.C.: First record of the Early Toarcian Oceanic Anoxic Event from the Southern Hemisphere, Neuquén Basin, Argentina, J. Geol. Soc. London, 167. 633−636, 2010.

Anderson, T.F. and Arthur, M.A.: Stable isotopes of oxygen and carbon and their application to sedimentologic and paleoenvironmental problems, in: Stable isotopes in sedimentary geology, edited by Arthur, M.A., SEPM Short Course 10, 1-1−1-151, 1983.

Anderson, T.F., Popp, B.N., Williams, A.C., Ho, L.Z. and Hudson, J.D.: The stable isotopic record of fossils from the Peterborough Member, Oxford Clay Formation (Jurassic), UK: palaeoenvironmental implications. J. Geol. Soc. London, 151. 125−138, 1994.

643 Armendáriz, M., Rosales, I., Bádenas, B., Aurell, M., García-Ramos, J.C. and Piñuela, L.:
644 High-resolution chemostratigraphic record from Lower Pliensbachian
645 belemnites: Palaeoclimatic perturbations, organic facies and water mass
646 Exchange (Asturian basin, northern Spain), Palaeogeogr. Palaeocl., 333–334,
647 178–191, 2012.

648 Bádenas, B, Aurell, M., García-Ramos, J.C., González, B. and Piñuela, L.: Sedimentary vs.
649 Diagenetic control on rhytmic calcareous successions (Pliensbachian of Asturias,
650 Spain), Terra Nova, 21, 162–170, 2009.

651 Bádenas, B, Aurell, M., Armendáriz, M., Rosales, I., García-Ramos, J.C. and Piñuela, L.:
652 Sedimentary and chemostratigraphic record of climatic cycles in Lower
653 Pliensbachian marl–limestone platform successions of Asturias (North Spain),
654 Sed. Geol., 281, 119–138, 2012.

655 Baeza-Carratalá, J.F., García Joral, F., Giannetti, A. and Tent-Manclús, J.E.: Evolution of
656 the last koninckinids (Athyrida, Koninckidae), a precursor signal of the early
657 Toarcian mass extinction event in the Western Tethys, Palaeogeogr. Palaeocl.,
658 429, 41–56, 2015.

659 Bailey, T.R., Rosenthal, Y., McArthur, J.M., van de Schootbrugge, B. and Thirlwall, M.F.:
660 Paleoceanographic changes of the Late Pliensbachian−Early Toarcian interval: a
661 possible link to the genesis of an Oceanic Anoxic event, Earth Planet. Sc. Lett.,
662 212, 307−320, 2003.

663 Benito, M.I. and Reolid, M.: Belemnite taphonomy (Upper Jurassic, Western Tethys)
664 part II: Fossil–diagenetic analysis including combined petrographic and
665 geochemical techniques, Palaeogeogr. Palaeocl., 358–360, 89–108, 2012.

666 Berner, R.A.: GEOCARB II: A revised model of atmospheric CO2 over Phanerozoic time.
667 Am. J Sci. 249, 56–41, 1994. A revised model of atmospheric CO2 over
668 Phanerozoic time, Am. J. Sci., 249, 56–41, 1994.

669 Berner, R.A.: GEOCARBSUL: a combined model for Phanerozoic atmospheric O_2 and
670 CO_2, Geochim. Cosmochim. Ac., 70, 5653–5664, 2006.

671 Berner, R.A. and Kothavala, Z. GEOCARB III. A revised model of atmospheric CO2 over
672 Phanerozoic time, Am. J. Sci., 301, 182–204, 2001.

673 Bettencourt, V. and Guerra, A.: Carbon- and Oxygen-isotope composition of the
674 cuttlebone of *Sepia officialis*: a tool for predicting ecological information, Mar.
675 Biol., 133, 651–657, 1999.

676 Bodin, S., Mattioli, E., Fröhlich, S., Marshall, J.D., Boutib, L.,Lahsini, S. and Redfern, J.:
677 Toarcian carbon isotope shifts and nutrient changes from the Northern margin
678 of Gondwana (High Atlas, Morocco, Jurassic): Palaeoenvironmental
679 implications, Palaeogeogr. Palaeocl., 297, 377−390, 2010.

680 Burgess, S.D. and Bowring, S.A., Fleming, T.H., Elliot, D.H.: High-precision
681 geochronology links the Ferrar large igneous province with early-Jurassic ocean
682 anoxia and biotic crisis, Earth. Planet. Sc. Lett., 415, 90−99, 2015.

683 Cecca, F.: Paleobiogeography of Tethyan ammonites during the Tithonian (latest
684 Jurassic), Palaeogeogr. Palaeocl., 147, 1–37, 1999

685 Chandler, M.A., Rind, D. and Ruedy, R.: Pangaean climate during the Early Jurassic:
686 GCM simulations and the sedimentary record of paleoclimate, Geol. Soc. Am.
687 Bull., 104, 543−559, 1992.

688 Clémence, M.E.: Pattern and timing of the Early Jurassic calcareous nannofossil crisis,
689 Palaeogeogr. Palaeocl., 411, 56–64, 2014.

690 Clémence, M.E., Gardin, S. and Bartolini A.: New insights in the pattern and timing of
691 the Early Jurassic calcareous nannofossil crisis, Palaeogeogr. Palaeocl., 427,
692 100–108, 2015.

693 Cohen, A.S., Coe, A.L., Harding, S.M. and Schwark, L.: Osmium isotope evidence for
694 regulation of atmospheric CO_2 by continental weathering. Geology, 32,
695 157−160, 2004

696 Comas-Rengifo, M.J. and Goy, A.: Caracterización biocronoestratigráfica del
697 Sinemuriense Superior y el Pliensbachiense entre los afloramientos de Playa de
698 Vega y de Lastres (Asturias), in: Las sucesiones margo-calcáreas marinas del
699 Jurásico Inferior y las series fluviales del Jurásico Superior. Acantilados de Playa
700 de Vega (Ribadesella), edited by: García-Ramos J.C. (Coord.), V Congreso
701 Jurásico de España, MUJA, 9−18, 2010.

702 Cortés, J.E.: La arquitectura deposicional de los carbonatos del Jurásico Inferior y
703 Medio relacionados con los materiales volcánicos del sureste de la Cordillera
704 Ibérica, PhD Thesis, Fac. Sci. Geol. Univ. Complutense Madrid, Spain, 2015.

705 Crame, J.A.: Bipolar molluscs and their evolutionary implications, J. Biogeogr., 20,
706 145–161, 1993.

707 Damborenea, S.E., Echevarria, J. and Ros Franch, S.: Southern Hemisphere
708 palaeobiogeography of Triassic–Jurassic marine bivalves, SpringerBriefs in Earth
709 System Sciences, 2013.

710 De Lurio, J.D. and Frakes, L.A.: Glendonites as a paleoenvironmental tool: Implications
711 for early Cretaceous high latitude climates in Australia, Geochim. Cosmochim.
712 Acta, 63, 1039−1048, 1999.

713 Dera, G., Pucéat, E., Pellenard, P., Neige, P., Delsate, D., Joachimski, M.M., Reisberg, L.
714 and Martinez, M.: Water mass exchange and variations in seawater
715 temperature in the NW Tethys during the Early Jurassic: Evidence from
716 neodymium and oxygen isotopes of fish teeth and belemnites, Earth. Planet. Sc.
717 Lett., 286, 198−207, 2009.

718 Dera, G., Neige, P., Dommergues, J.L., Fara, E., Lafont, R. and Pellenard, P.: High-
719 resolution dynamics of Early Jurassic marine extinctions: the case of
720 Pliensbachian−Toarcian ammonites (Cephalopoda), J. Geol. Soc. London, 167,
721 21−33, 2010.

722 Dera, G., Brigaud, B., Monna, F., Laffont, R., Pucéat, E., Deconinck, J.F., Pellenard, P.,
723 Joachimski, M.M. and Durlet, C.: Climatic ups and downs in a disturbed Jurassic
724 world, Geology, 39, 215−218, 2011.

725 Devyatov, V.P., Knyazev, V.G., Nikitenko, B.L. and Glinskikh, L.A.:
726 Pliensbachian−Toarcian boundary in northeastern Siberia and stratigraphic
727 position of the Kurung Mb of the Kelimyar Formation (Kelimyar River. Olenek
728 River basin), Otechestvennaya Geol. 5, 105−112, 2010.

729 Dommergues, J.L., Meister, Ch. and Mouterde, R.: 3.–Pliensbachiense, edited by
730 Cariou, E., Hantzpergue, P., Bull. Centre Rech. Elf Explor. Prod. Pau, 17, 15–23,
731 1997.

732 Dromart, G., Garcia, J.-P., Picard, S., Atrops, F., Lécuyer, C. and Sheppard, S.M.F.: Ice
733 age at the Middle–Late Jurassic transition?, Earth. Planet. Sc. Lett., 213,
734 205−220, 2003.

735 Elmi, S., Rulleau, L., Gabilli, J. and Mouterde, R.: Toarcien. Bioestratigraphie Jurassique
736 ouest-européen méditerranéen: zonations parallèles et distribution des
737 invertébrés et microfossils, edited by Cariou, E. and Hantzpergue, P., Bull.
738 Centre Rech. Elf Explor. Prod., Pau, 17, 25–36, 1997.

739 Enay, R. and Cariou, E.: Ammonite faunas and palaeobiogeography of the Himalayan
740 belt during the Jurassic: initiation of a late Jurassic Austral ammonite fauna,
741 Palaeogeogr. Palaeocl., 134, 1−38, 1997.

742 Fraguas, A.: Late Sinemurian−Early Toarcian calcareous nannofosils from the
743 Cantabrian Basin: spatial and temporal distribution, PhD thesis, Fac. Sci. Geol.
744 Univ. Complutense Madrid, Spain, 2010.

745 Fraguas, A., Comas-Rengifo, M.J., Gómez, J.J. and Goy, A.: The calcareous nannofossil
746 crisis in Northern Spain (Asturias province) linked to the Early Toarcian
747 warming-driven mass extinction, Mar. Micropaleontol., 94–95, 58–71, 2012.

748 Frakes, L.A., Francis, J.E. and Syktus, J.I.: Climate models of the Phanerozoic, Cambridge
749 University Press. Cambridge, 274 pp, 1992.

750 Francheschi, M., Dal Corso, J., Posenato, R., Roghi, Masetti, D. and Jenkyns, H.C.: Early
751 Pliensbachian (Early Jurassic) C-isotope perturbation and the diffusion of the
752 Lithiotis Fauna: Insights from the western Tethys, Palaeogeogr. Palaeocl., 410,
753 255−263, 2014.

754 García Joral, F., Gómez, J.J. and Goy, A.: Mass extinction and recovery of the Early
755 Toarcian (Early Jurassic) brachiopods linked to climate change in northern and
756 central Spain, Palaeogeogr. Palaeocl., 302, 367–380, 2011.

757 Gómez, J.J. and Arias, C.: Rapid warming and ostracods mass extinction at the Lower
758 Toarcian (Jurassic) of central Spain, Mar. Micropaleontol., 74, 119−135, 2010.

759 Gómez, J.J. and Goy, A.: Warming-driven mass extinction in the Early Toarcian (Early
760 Jurassic) of northern Spain. Correlation with other time-equivalent European
761 sections, Palaeogeogr. Palaeocl., 306, 176−195, 2011.

762 Gómez, J.J., Goy, A. and Canales, M.L.: Seawater temperature and carbon isotope
763 variations in belemnites linked to mass extinction during the Toarcian (Early
764 Jurassic) in Central and Northern Spain. Comparison with other European
765 sections, Palaeogeogr. Palaeocl., 258, 28−58, 2008.

766 Goy, A., Comas-Rengifo, M.J., García-Ramos, J.C., Gómez, J.J., Herrero, C., Suárez-Vega,
767 L.C. and Ureta, M.: The Toarcian Stage in Asturias (North Spain): Ammonites
768 record, stratigraphy and correlations, Earth Sci. Frontiers, Spec. Publ., 17,
769 38−39, 2010a.

770 Goy, A., Comas-Rengifo, M.J., Gómez, J.J., Herrero, C., Suárez-Vega, L.C. and Ureta, M.:
771 Biohorizontes de ammonoideos del Toarciense en Asturias, edited by Ruiz
772 Omeñaca, J.J., Piñuelas, L. and García-Ramos J.C., Com. V Congreso Jurásico de
773 España, MUJA, 94−102, 2010b.

774 Guex, J.: Aperçu biostratigraphique sur le Toarcien inférieur du Moyen-Atlas marocain
775 et discussion sur la zonation de ce sous-étage dans les séries
776 méditerranéennes, Eclogae Geol. Helv., 66, 495−523, 1973.

777 Guex, J., Morard, A., Bartolini, A. and Morettini, E.: Découverte d'une importante
778 lacune stratigraphique à la limite Domérien-Toarcien: implications paléo-
779 océnographiques, Bull. Soc. Vaud. Sc. Nat., 87, 277−284, 2001.

780 Guex, J., Bartolini, A., Spangenberg, J., Vicente, J.C. and Schaltegger, U.: Ammonoid
781 multi-extinction crises during the Late Pliensbachian−Toarcian and carbon cycle
782 instabilities, Solid Earth Discuss., 4, 1205−1228, doi:10.5194/sed-4-1205-2012,
783 2012.

784 Hallam, A.: Diversity and density characteristics of Pliensbachian−Toarcian molluscan
785 and brachiopod faunas of the North Atlantic margins, Lethaia, 4, 389−412,
786 1972.

787 Hallam, A.: Jurassic environments, Cambridge Earth Sci. Ser., Cambridge University
788 Press, Cambridge, 269 pp. 1975.

789 Hallam, A.: Jurassic climates as inferred from the sedimentary and fossil record, Philos.
790 T. R. Soc. B, 342, 287–296, 1993.

791 Harazim, D., van de Schootbrugge, B., Sorichter, K., Fiebig, J., Weug, A., Suan, G. and
792 Oschmann, W.: Spatial variability of watermass conditions within the European
793 Epicontinental Seaway during the Early Jurassic (Pliensbachian–Toarcian),
794 Sedimentology, 60, 359–390, 2013.

795 Hesselbo, S.P., Gröcke, D.R., Jenkyns, H.C., Bjerrum, C.J., Farrimond, P., Morgans Bell,
796 H.S. and Green, O.R.: Massive dissociation of gas hydrate during a Jurassic
797 oceanic anoxic event. Nature, 406, 392−395, 2000.

798 Hesselbo, S.P., Meister, C. and Gröcke, D.R.: A potential global stratotype for the
799 Sinemurian–Pliensbachian-boundary (Lower Jurassic), Robin Hood's Bay, UK;
800 ammonite faunas and isotope stratigraphy, Geol. Mag., 137, 601–607, 2000.

801 Hesselbo, S.P., Jenkyns, H.C., Duarte, L.V. and Oliveira, L.C.V.: Carbon-isotope record of
802 the Early Jurassic (Toarcian) Oceanic Anoxic Event from fossil wood and marine
803 carbonate (Lusitanian Basin, Portugal), Earth Planet. Sc. Lett., 253, 455−470,
804 2007.

805 Jansen, J.H.F., Woensdregt, C.F., Kooistra, M.J. and van der Gaast, S.J.: Ikaite
806 pseudomorphs in the Zaire deep-sea fan: an intermediate between calcite and
807 porous calcite, Geology, 15, 245–248, 1987.

808 Jenkyns, H.C.: Evidence for rapid climate change in the Mesozoic-Palaeogene
809 greenhouse world, Philos. T. R. Soc. A, 361, 1885−1916, 2003.

810 Jenkyns, H.C. and Clayton, C.J.: Lower Jurassic epicontinental carbonates and
811 mudstones from England and Wales: chemostratigraphic signals and the early
812 Toarcian anoxic event, Sedimentology, 44, 687−706, 1997.

813 Jenkyns, H.C., Jones, C.E., Gröcke, D.R., Hesselbo, S.P. and Parkinson, D.N.:
814 Chemostratigraphy of the Jurassic System: application, limitations and
815 implications for palaeoceanography, J. Geol. Soc. London, 159, 351−378, 2002.

816 Jenkyns, H.C. and Weedon, G.P.: Chemostratigraphy ($CaCO_3$, TOC, $\delta^{13}C_{org}$) of
817 Sinemurian (Lower Jurassic) black shales from the Wessex Basin, Dorset and
818 palaeoenvironmental implications, Newsl. on Stratigr., 46, 1−21, 2013.

819 Jourdan, F., Féraud, G., Bertrand, H., Watkeys, M.K. and Renne, P.R.: Distinct brief
820 major events in the Karoo large igneous province clarified by new $^{40}Ar/^{39}Ar$
821 ages on the Lesotho basalts, Lithos, 98, 195−209, 2007.

822 Jourdan, F., Féraud, G., Bertrand, H., Watkeys, M.K. and Renne, P.R.: The new $^{40}Ar/^{39}Ar$
823 ages of the sill complex of the Karoo large igneous province: Implications for
824 the Pliensbachian–Toarcian climate change, Geochem. Geophy. Geosy., 9,
825 1−29, Q06009,doi: 10.1029/2008GC001994, 2008

826 Kaplan, M.E.: Calcite pseudomorphoses in Jurassic and Lower Cretaceous deposits of
827 the Northern Area of Eastern Liberia, Geol. Geofiz., 19, 62−70, 1978.

828 Kemp, D.B., Coe, A.L., Cohen, A.S. and Schwark, L.: Astronomical pacing of methane
829 release in the Early Jurassic period, Nature 437, 396−399, 2005.

830 Kidder, D.L. and Worsley, T.R., Phanerozoic Large Igneous Province (LIPs): HEATT
831 (Haline Euxinic Acidic Thermal Transgression) episodes, and mass extinctions,
832 Palaeogeogr. Palaeocl., 295, 162−191, 2010.

833 Korte, C. and Hesselbo, S.P.: Shallow marine carbon and oxygen isotope and elemental
834 records indicate icehouse–greenhouse cycles during the Early Jurassic,
835 Paleoceanography, 26, PA 4219, doi: 10.1029/2011PA002160, 2011.

836 Kump, L.R. and Arthur, M.A.: Interpreting carbon-isotope excursions: carbonates and
837 organic matter, Chem. Geol., 161, 181−198, 1999.

838 Li, Q., McArthur, J.M., and Atkinson, T.C.: Lower Jurassic belemnites as indicators of
839 palaeo-temperature, Palaeoclimatol. Palaeoecol., 315−316, 38−45, 2012.

840 Littler, K., Hesselbo, S.P. and Jenkyns, H.C.: A carbon-isotope perturbation at the
841 Pliensbachian−Toarcian boundary: evidence from the Lias Group, NE England,
842 Geol. Mag., 147, 181−192, 2010.

843 Liu, C., Heinze, M. and Fürsich, F.T.: Bivalve provinces in the Proto-Atlantic and along
844 the southern margin of the Tethys in the Jurassic, Palaeogeogr. Palaeocl., 137,
845 127−151, 1998.

846 McArthur, J.M., Donovan, D.T., Thirlwall, M.F., Fouke, B.W. and Mattey, D.: Strontium
847 isotope profile of the early Toarcian (Jurassic) oceanic anoxic event, the
848 duration of ammonite biozones, and belemnite palaeotemperatures, Earth.
849 Planet. Sc. Lett., 179, 269−285, 2000.

850 McArthur, J.M., Doyle, P., Leng, M.J., Reeves, K., Williams, T., García-Sanchez, R. and
851 Howart, R.J.: Testing palaeo-environmental proxies in Jurassic belemnites:
852 Mg/Ca, Sr/Ca, Na/Ca, $\delta^{18}O$ and $\delta^{13}C$, Palaeogeogr. Palaeocl., 252, 464−480,
853 2007.

854 McElwain, J.C., Wade-Murphy, J. and Hesselbo, S.P.: Changes in carbon dioxide during
855 an oceanic anoxic event linked to intrusion into Gondwana coals. Nature, 435,
856 479−482, 2005.

857 Metodiev, L. and Koleva-Rekalova, E.: Stable isotope records ($\delta^{18}O$ and $\delta^{13}C$) of Lower-
858 Middle Jurassic belemnites from the Western Balkan mountains (Bulgaria):
859 Palaeoenvironmental application, Appl. Geochem., 23, 2845−2856, 2008.

860 Mitchel, S.F.: Eight belemnite biohorizons in the Cenomanioan of northwest Europe
861 and their importance. Geol. J., 40, 363−382, 2005.

862 Moulin, M., Fluteau, F., Courtillot, V., Marsh, J., Delpech, G. and Quidelleur, X.: An
863 attempt to constrain the age, duration and eruptive history of the Karoo flood
864 basalt: Nande's Nek section (South Africa), J. Geophys. Res., 116, B07403, doi:
865 10.1029/2011JB008210. 2011.

866 Mutterlose, J., Malkoc, M., Schouten, S., Sinninghe Damsté, J.S. and Foster, A.: TEX_{86}
867 and stable $\delta^{18}O$ paleothermometry of early Cretaceous sediments: Implications
868 for belemnite ecology and palaeotemperature proxy application. Earth Planet.
869 Sc. Lett., 298, 286−298, 2010.

870 Nikitenko, B.L.: The Early Jurassic to Aalenian paleobiogeography of the arctic realm:
871 Implication of microbenthos (foraminifers and ostracodes), Stratigr. Geol.
872 Correl., 16, 59–80, 2008.

873 Ogg, J.G.: The Jurassic Period, in: A Geologic Time Scale 2004, edited by Gradstein,
874 F.M., Ogg, J.G. and Smith, A., Cambridge University Press, Cambridge, pp.
875 307−343, 2004.

876 Ogg, J.G. and Hinnov, L.A.: Jurassic, in: The Geologic Time Scale 2012, edited by
877 Gradstein, F.M., Ogg, J.G., Schmitz, M. and Ogg, G.,. Elsevier B.V. Amsterdam,
878 731−791, 2012.

879 Osete, M.L., Gómez, J.J., Pavón-Carrasco, F.J., Villalaín, J.J., Palencia, A., Ruiz-Martínez,
880 V.C. and Heller, F.: The evolution of Iberia during the Jurassic from
881 palaeomagnetic data, Tectonophysics, 50, 105–120, 2010.

882 Page, K.N.: The Lower Jurassic of Europe: its subdivision and correlation, Geol. Survey
883 Denmark and Greeland Bull., 1, 23−59, 2003.

884 Page, K.N.: The evolution and geography of Jurassic ammonoids, P. Geol. Assoc. Can.,
885 119, 35−57, 2008.

886 Payne, J.L. and Kump, L.R.: Evidence for recurrent Early Triassic massive volcanism
887 from quantitative interpretation of carbon isotope fluctuations, Earth Planet.
888 Sc. Lett., 256, 264−277, 2007.

889 Percival, L.M.E., Witt, M.L.I., Mather, T.A., Hermoso, M., Jenkyns, H.C., Hesselbo, S.P.,
890 Al-Suwaidi, A.H., Storm, M.S., Xu, W. and Ruhl, M.: Globally enhanced mercury
891 deposition during the end-Pliensbachian and Toarcian OAE: A link to the Karoo-
892 Ferrar Large Igneous Province. Earth Planet. Sc. Lett. 428, 267–280, 2015.

893 Price, G.D.: The evidence of polar ice during the Mesozoic, Earth Sci. Rev., 48, 183−210,
894 1999.

895 Price, G. D., Twitchett, R.J., Smale, C. and Marks, V.: Isotopic analysis of the life history
896 of the enigmatic squid *Spirula spirula*, with implications for studies of fossil
897 cephalopods, Palaios, 24, 273−279, 2009.

898 Philippe, M. and Thevenard, F.: Distribution and palaeoecology of the Mesozoic wood
899 genus *Xenoxylon*: palaeoclimatological implications for the Jurassic of western
900 Europe, Rev. Palaeobot. Palyno., 91, 353−370, 1996.

901 Quesada, S., Robles, S. and Rosales, I.: Depositional architecture and transgressive–
902 regressive cycles within Liassic backstepping carbonate ramps in the Basque–
903 Cantabrian Basin, northern Spain, J. Geol. Soc. London, 162, 531–548, 2005.

904 Rees, P.A., Zeigler, A.M. and Valdes, P.J.: Jurassic phytogeography and climates: new
905 data and model comparisons, in: Warm climates in Earth History, edited by
906 Huber, B., Macleod, K., Wing, S., Cambridge University Press, Cambridge, 297–
907 318, 1999.

908 Retallack, G.J.: Greenhouse crises of the past 300 million years, Geol. Soc. Am. Bull.,
909 121, 1441–1455, 2009.

910 Rexfort, A. and Mutterlose, J.: The role of biogeography and ecology on the isotope
911 signature of cuttlefishes (Cephalopoda, Sepiidae) and the impact on belemnite
912 studies, Palaeogeogr. Palaeocl., 244, 212–221, 2009.

913 Rogov, M.A. and Zakharov, V.A.: Jurassic and Lower Cretaceous glendonite occurrences
914 and their implication for Arctic paleoclimate reconstructions and stratigraphy,
915 Earth Sci. Frontiers. Spec. Issue., 17, 345–347, 2010.

916 Röhl, H.J., Schmid-Röhl, A., Oschmann, W., Frimmel, A. and Schwark, L.: The Posidonia
917 Shale (Lower Toarcian) of SW-Germany: an oxygen-depleted ecosystem
918 controlled by sea level and palaeoclimate, Palaeogeogr. Palaeocl., 165, 27−52,
919 2001.

920 Rosales, I., Quesada, S. and Robles, S.: Primary and diagenetic isotopic signal in fossils
921 and hemipelagic carbonates: the lower Jurassic of northern Spain,
922 Sedimentology, 48, 1149–1169, 2001.

923 Rosales, I., Quesada, S. and Robles, S.: Paleotemperature variations of Early Jurassic
924 seawater recorded in geochemical trends of belemnites from the
925 Basque−Cantabrian basin, northern Spain, Palaeogeogr. Palaeocl., 203,
926 253−275, 2004.

927 Sælen, G., Doyle, P. and Talbot, M.R.: Stable-Isotope Analyses of Belemnite Rostra
928 from the Whitby Mudstone Fm., England: Surface Water Conditions during
929 Deposition of a Marine Black Shale, Palaios, 11, 97−117, 1996.

930 Schmid-Röhl, A., Röhl, H.J., Oschmann, W., Frimmel, A. and Schwark, L.:
931 Palaeoenvironmental reconstruction of Lower Toarcian epicontinental black
932 shales (Posidonia Shale, SW Germany): global versus regional control, Geobios,
933 35, 13−20, 2002.

934 Schouten, S., van Kaam-Peters, H.M.E., Rijpstra, W.I.C., Schoell, M. and Sinninghe
935 Damste, J.S.: Effects of an oceanic anoxic event on the stable carbon isotopic
936 composition of Early Toarcian carbon, Am. J. Sci., 300, 1−22, 2000.

937 Sell, B., Ovtcharova, M., Guex, J., Bartolini, A., Jourdan, F., Spangenberg, J.E., Vicente,
938 J.C. and Schaltegger, U.: Evaluating the temporal link between the Karoo LIP
939 and climatic-biologic events of the Toarcian Stage with high-precision U–Pb
940 geochronology, Earth Planet. Sc. Lett., 408, 48–56, 2014.

941 Selleck, B.W., Carr, P.F. and Jones, B. G.: A review and synthesis of glendonites
942 (pseudomorphs after ikaite) with new data: Assessing applicability as recorders
943 of ancient coldwater conditions, J. Sedimentary Res., 77, 980–991, 2007.

944 Sellwood, B.W. and Valdes, P.J.: Jurassic climates, P. Geol. Assoc. Can., 119, 5–17,
945 2008.

946 Shackleton, N. J. and Kenett, J. P.: Paleotemperature history of the Cenozoic and the
947 initiation of Antarctic glaciation: Oxygen and carbon isotope analysis in DSDP
948 sites 277, 279 and 281, in: Initial Reports of the Deep Sea Drilling Projects, 29,
949 edited by: Kennet, J. P., Houtz, R. E., Andrews, P. B., Edwards, A. R., Gosting, V.

A., Hajós, M., Hampton, M. A., Jenkins, D.G., Margolis, S. V., Ovenshine, A. T., and Perch-Nielsen, K., US Government Printing Office,Washington, 743–756, 1975.

Silva, R.L., Duarte, L.V., Comas-Rengifo, M.J., Mendonça Filho, J.G. and Azerêdo, A.C.: Update of the carbon and oxygen isotopic records of the Early–late Pliensbachian (Early Jurassic, ~187Ma): insights from the organic-rich hemipelagic series of the Lusitanian Basin (Portugal), Chem. Geol., 283, 177–184. 2013.

Steinthorsdottir, M. and Vajda, V.: Early Jurassic (late Pliensbachian) CO_2 concentrations based on stomatal analysis of fossil conifer leaves from eastern Australia, Gondwana Res., 27, 829–897, 2015.

Stevens, G.R. and Clayton, R.N.: Oxygen isotopes studies on Jurassic and Cretaceous belemnites from New Zealand and their biogeographic significance, New. Zeal.J. Geol. Geop., 14, 829–897, 1971.

Suan, G., Mattioli, E., Pittet,B., Maillot, S. and Lécuyer, C.: Evidence for major environmental perturbation prior to and during the Toarcian (Early Jurassic) Oceanic Anoxic Event from the Lusitanian Basin, Portugal, Paleoceanography 23, 1202, doi: 10.1029/2007PA001459, 2008.

Suan, G., Mattioli, E., Pittet,B., Lécuyer, C., Suchéras-Marx, B., Duarte, L.V., Philippe, M., Reggiani, F. and Martineau, F.: Secular environmental precursor to Early Toarcian (Jurassic) extreme climate changes, Earth Planet. Sc. Lett., 290, 448–458, 2010.

Suan, G., Nikitenko, B., Rogov, M.A., Baudin, F., Spangenberg, J.E., Knyazev, V.G., Glinskikh, L.A., Goryacheva, A.A., Adatte, T., Riding, J., Föllmi, K.B., Pittet, B.,Mattioli, E. and Lécuyer, C.: Polar record of Early Jurassic massive carbon injection, Earth Planet. Sc. Lett., 312, 102−113, 2011.

Suárez-Vega, L.C.: Estratigrafía del Jurásico en Asturias, Cuad. Geol. Ibérica, 3, 1−369, 1974.

Svensen, H., Planke, S., Chevalier, L., Malthe-Sørenssen, A., Corfu, F. and Jamtveit, B.: Hydrothermal venting of greenhouse gasses triggering Early Jurassic global warming, Earth Planet. Sc. Lett., 256, 554−566, 2007.

Teichert, B.M.A. and Luppold, F.W.: Glendonites from an Early Jurassic methane seep−Climate or methane indicators?, Palaeogeogr. Palaeocl., 390, 81−93, 2013.

Ullmann, C.V. and Korte, C.: Diagenetic alteration in low-Mg calcite from macrofossils: a review, Geol. Q., 59, 3–20, 2015.

Ullmann, C.V., Thibault, N., Ruhl, M., Hesselbo, S.P. and Korte, C.: Effect of a Jurassic oceanic anoxic event on belemnite ecology and evolution, P. Nat. Acad. Sci. USA, 111, 10073–10076, 2014.

Valenzuela, M.: Estratigrafía, sedimentología y paleogeografía del Jurásico de Asturias, Ph. D. Thesis, Fac. Sci. Geol. Univ. Oviedo, Spain, 1988.

van de Schootbrugge, Harazim, D., Sorichter, K., Oschmann, W., Fiebig, J., Püttmann, W., Peinl, M., Zanella, F., Teichert, B.M.A., Hoffmann, Stadnitskaia, J.A. and Roshental, Y.: The enigmatic ichnofossil Tisoa siphonalis and widespread authigenic seep carbonate formation during the Late Pliensbachian in southern France, Biogeosciences, 7, 3123–3138, doi: 10.5194/bg-7-3123-2010, 2010.

Wierzbowski, H. and Joachimski, M.M.: Reconstruction of Late Bajocian−Bathonian marine palaeoenvironments using carbon and oxygen isotope ratios of calcareous fossils from the Polish Jura Chain (central Poland). Palaeogeogr. Palaeocl., 254, 523−540, 2007.

Wigley, T.M.L., Richels, R. and Edmonds, J.A.: Economic and environmental choices in the stabilization of atmospheric CO_2 concentrations, Nature, 379, 240−243, 1996.

Woodfine, R.G., Jenkyns, H.C., Sarti, M., Baroncini, F. and Violante, C.: The response of two Tethyan carbonate platforms to the early Toarcian (Jurassic) oceanic anoxic event: environmental change and differential subsidence, Sedimentology, 55, 1011−1028, 2008.

Zakharov, V.A., Shurygin, B.N., Il'ina, V.I. and Nikitenko, B.L.: Pliensbachian−Toarcian biotic turnover in North Siberia and the Artic Region, Stratigr. Geol. Correl., 14, 399−417, 2006.

FIGURE CAPTIONS

Fig. 1. Location maps of the Rodiles section. (a): Sketched geological map of Iberia showing the position of the Asturian Basin. (b): Outcrops of the Jurassic deposits in the Asturian and the western part of the Basque−Cantabrian basins, and the position of the Rodiles section. (c): Geological map of the Asturian Basin showing the distribution of the different geological units and the location of the Rodiles section.

Fig. 2. Thick sections photomicrographs of some of the belemnites sampled for stable isotope analysis from the Upper Sinemurian and Pliensbachian of the Rodiles section. The unaltered by diagenesis non luminescent sampling areas (SA), where the samples have been collected, are indicated. A and B Sample ER 351, Late Sinemurian Raricostatum Chronozone, Aplanatum Subchronozone. A: optical transmitted light microscope, showing the carbonate deposit filling the alveolous (Cf), the outer rostrum cavum wall (Cw) and fractures (Fr). B: cathodoluminescence microscope photomicrograph, showing luminescence in the carbonate deposit filling the alveolous (Cf), in the outer rostrum cavum wall (Cw) and in the fractures (Fr). SA represents the unaltered sampling area. C and D: Sample ER 337, Early Pliensbachian Jamesoni Chronozone, Taylori-Polymorphus Subchronozones. C: optical transmitted light

microscope, showing fractures (Fr). D: cathodoluminescence microscope photomicrograph, showing luminescence in stylolites (St). SA is the unaltered sampling area. E and F: Sample ER 589a Early Pliensbachian Margaritatus Chronozone, Subnodosus Subchronozone. E: cathodoluminescence microscope, showing luminescence in the apical line (Ap), fractures (Fr) and stylolites (St). This area of the section was not suitable for sampling. F: another field of the same sample as H showing scarce fractures (Fr) and the unaltered not luminescent sampled area (SA). G and H: Sample ER 549a, Late Pliensbachian Margaritatus Chronozone, Stokesi Subchronozone. G: cathodoluminescence microscope showing luminescent growth rings (Gr) and stylolites (St). Area not suitable for sampling. H: cathodoluminescence microscope photomicrograph, of the same sample as G, showing luminescent growth rings (Gr) and fractures (Fr), with unaltered sampling area (SA). I: Sample ER 555 Late Pliensbachian Margaritatus Chronozone, Stokesi Subchronozone. Cathodoluminescence microscope photomicrograph showing luminescent growth rings (Gr) and the unaltered sampling area (SA). J and K: Sample ER 623 Late Pliensbachian Spinatum Chronozone, Apyrenum Subchronozone. J: cathodoluminescence microscope photomicrograph showing luminescent stylolites (St). K: Another field of the same sample as J showing luminescence in the apical line (Ap) and fractures (Fr) as well as the non luminescent unaltered sampling area (SA). L: Sample ER 597, Late Pliensbachian Margaritatus Chronozone, Gibbosus Subchronozone. Cathodoluminescence microscope photomicrograph showing luminescent carbonate deposit filling the alveolous (Cf), the outer and inner rostrum cavum wall (Cw), the fractures (Fr) and the non luminescent sampling area (SA). Scale in bar for all the photomicrographs: 1mm.

Fig. 3. Cross-plot of the $\delta^{18}O_{bel}$ against the $\delta^{13}C_{bel}$ values obtained in the Rodiles section showing a cluster type of distribution. All the assayed values are within the rank of normal marine values, and the correlation coefficient between both stable isotope values is negative, supporting the lack of diagenetic overprints in the sampled belemnite calcite. $\delta^{18}O_{bel}$ and $\delta^{13}C_{bel}$ in PDB.

Fig 4. Sketch of the stratigraphical succession of the uppermost Triassic and the Jurassic deposits of the Asturian Basin. The studied interval corresponds to the lower part of the Santa Mera Member of the Rodiles Formation. Pli.=Pliensbachian, Toar.= Toarcian. Aal.= Aalenian. Baj.=Bajocian.

Fig. 5. Stratigraphical succession of the Upper Sinemurian, the Pliensbachian and the Lower Toarcian deposits of the Rodiles section, showing the lithological succession, the ammonite taxa distribution, as well as the profiles of the $\delta^{18}O_{bel}$ and $\delta^{13}C_{bel}$ values obtained from belemnite calcite. $\delta^{18}O_{bel}$ and $\delta^{13}C_{bel}$ in PDB. Chronozones abbreviations: TEN: Tenuicostatum. Subchronozones abbreviations: RA: Raricostatum. MC: Macdonnelli. AP: Aplanatum. BR: Brevispina. JA: Jamesoni. MA: Masseanum. LU:

Luridum. MU: Maculatum. CA: Capricornus. FI: Figulinum. ST: Stokesi. HA: Hawskerense. PA: Paltum. SE: Semicelatum. EL: Elegantulum. FA: Falciferum.

Fig. 6. Correlation chart of the belemnite calcite-based $\delta^{13}C$ sketched curves across Western Europe. The earliest isotopic event is the Late Sinemurian $\delta^{13}C$ positive excursion, followed by the Early Pliensbachian negative excursion and the Ibex–Davoei positive peak. The Late Pliensbachian $\delta^{13}C$ positive excursion is bounded by a $\delta^{13}C$ negative peak, located around the Pliensbachian–Toarcian boundary. A significant $\delta^{13}C$ positive excursion is recorded in the Early Toarcian. $\delta^{13}C_{bel}$ values in PDB. . Chronozones abbreviations: TEN: Tenuicostatum. SER: Serpentinum.

Fig. 7. Curve of seawater palaeotemperatrures of the Late Sinemurian, Pliensbachian and Early Toarcian, obtained from belemnite calcite in the Rodiles section of Northern Spain. Two warming intervals corresponding to the Late Sinemurian and the Early Pliensbachian are followed by an important cooling interval, developed at the Late Pliensbachian, as well as a (super)warming event recorded in the Early Toarcian. Chronozones abbreviations: RAR: Raricostatum. D: Davoei. TENUICOSTA.: Tenuicostatum. Subchronozones abbreviations: DS: Densinodulum. RA: Raricostatum. MC: Macdonelli. AP: Aplanatum. BR: Bevispina. JA: Jamesoni. VA: Valdani. LU: Luridum. CA: Capricornus. FI: Figulinum. SU: Subnodosus. PA: Paltum. SE: Semicelatum. FA: Falciferum.

Fig. 8. Correlation chart of the belemnite calcite-based $\delta^{18}O$ sketched curves obtained in different areas of Western Europe. Several isotopic events along the latest Sinemurian, Pliensbachian and Early Toarcian can be recognized. The earliest event is a $\delta^{18}O$ negative excursion corresponding to the Late Sinemurian Warming. After an interval of “normal” $\delta^{18}O$ values developed in most of the Jamesoni Chronozone and the earliest part of the Ibex Chronozone, another $\delta^{18}O$ negative excursion was developed in the Ibex, Davoei and earliest Margaritatus chronozones, representing the Early Pliensbachian Warming interval. A main $\delta^{18}O$ positive excursion is recorded at the Late Pliensbachian and the earliest Toarcian in all the correlated localities, representing the important Late Pliensbachian Cooling interval. Another prominent $\delta^{18}O$ negative shift is recorded in the Early Toarcian. Values are progressively more negative in the Tenuicostatum Chronozone and suddenly decrease around the Tenuicostatum–Serpentinum zonal boundary, delineating the Early Toarcian $\delta^{18}O$ negative excursion which represents the Early Toarcian (super)Warming interval. $\delta^{18}O_{bel}$ values in PDB.

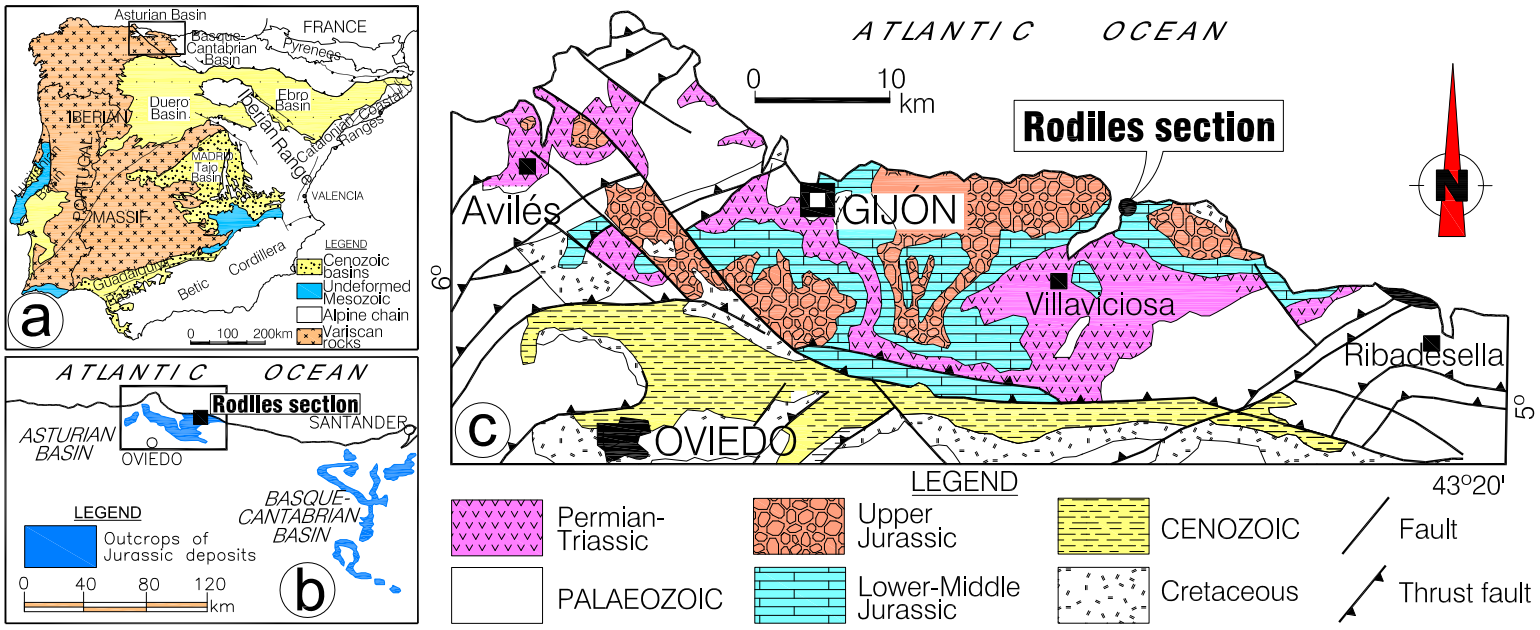

Fig. 1. Gómez, Comas-Rengifo and Goy

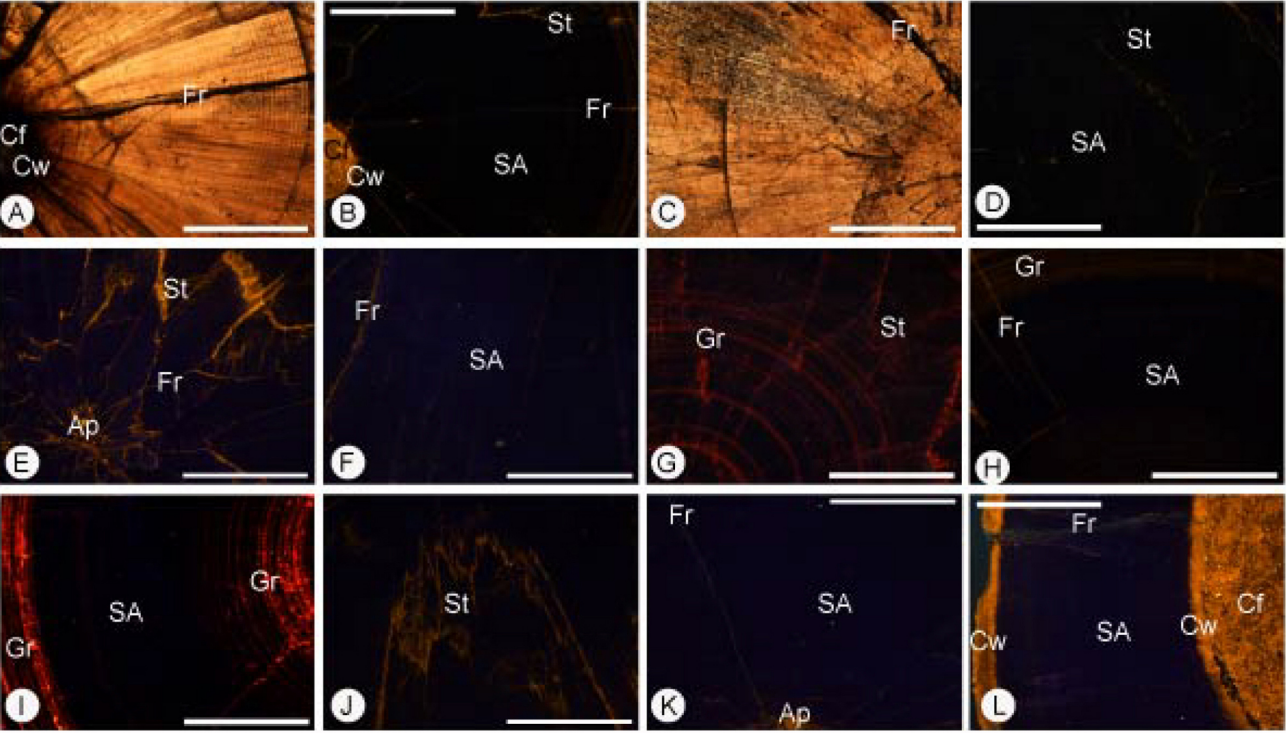

Fig 2. Gómez, Comas and Goy

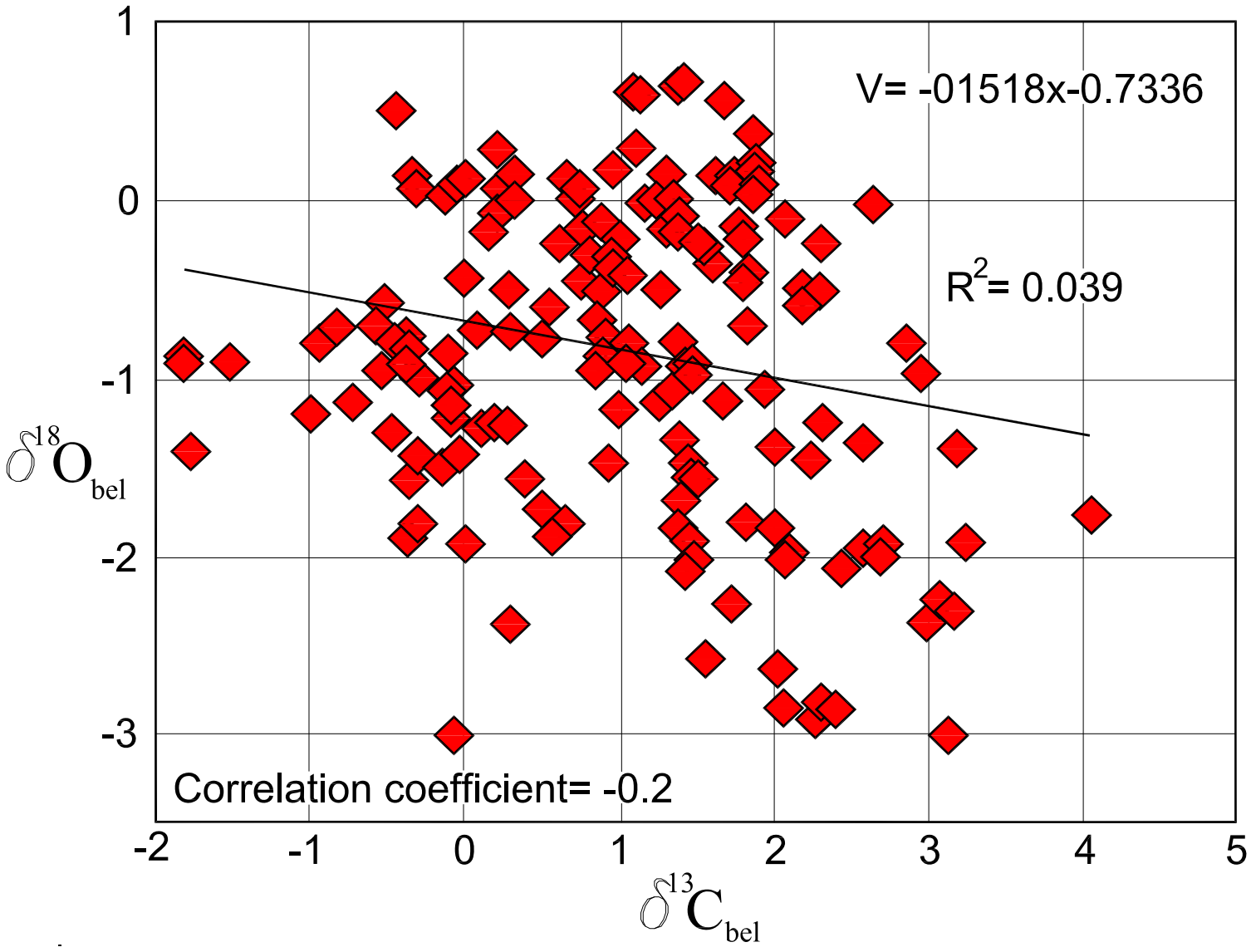

Fig. 3. Gómez, Comas-Rengifo and Goy

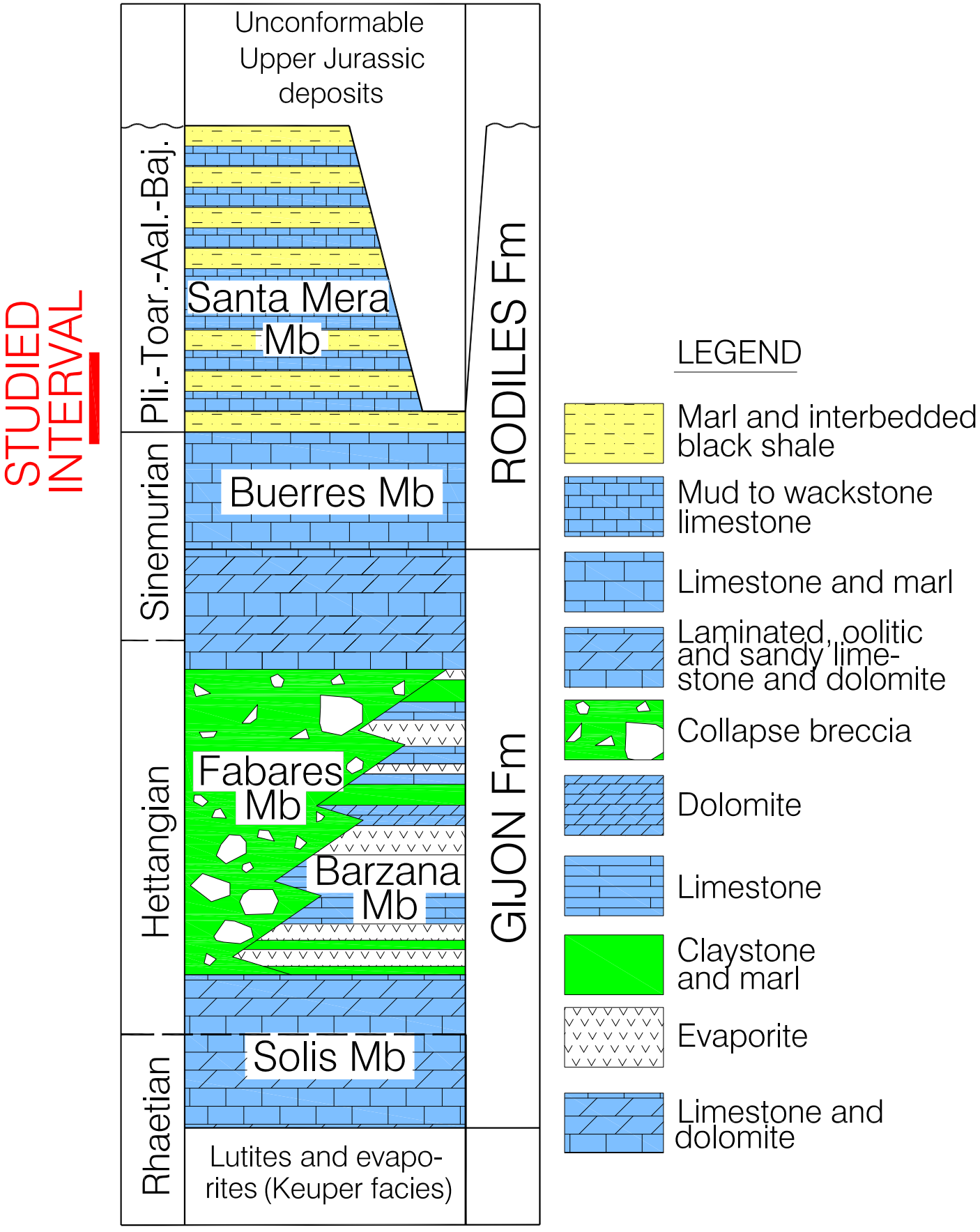

Fig. 4. Gómez, Comas-Rengifo and Goy

Fig. 5. Gómez, Comas-Rengifo and Goy

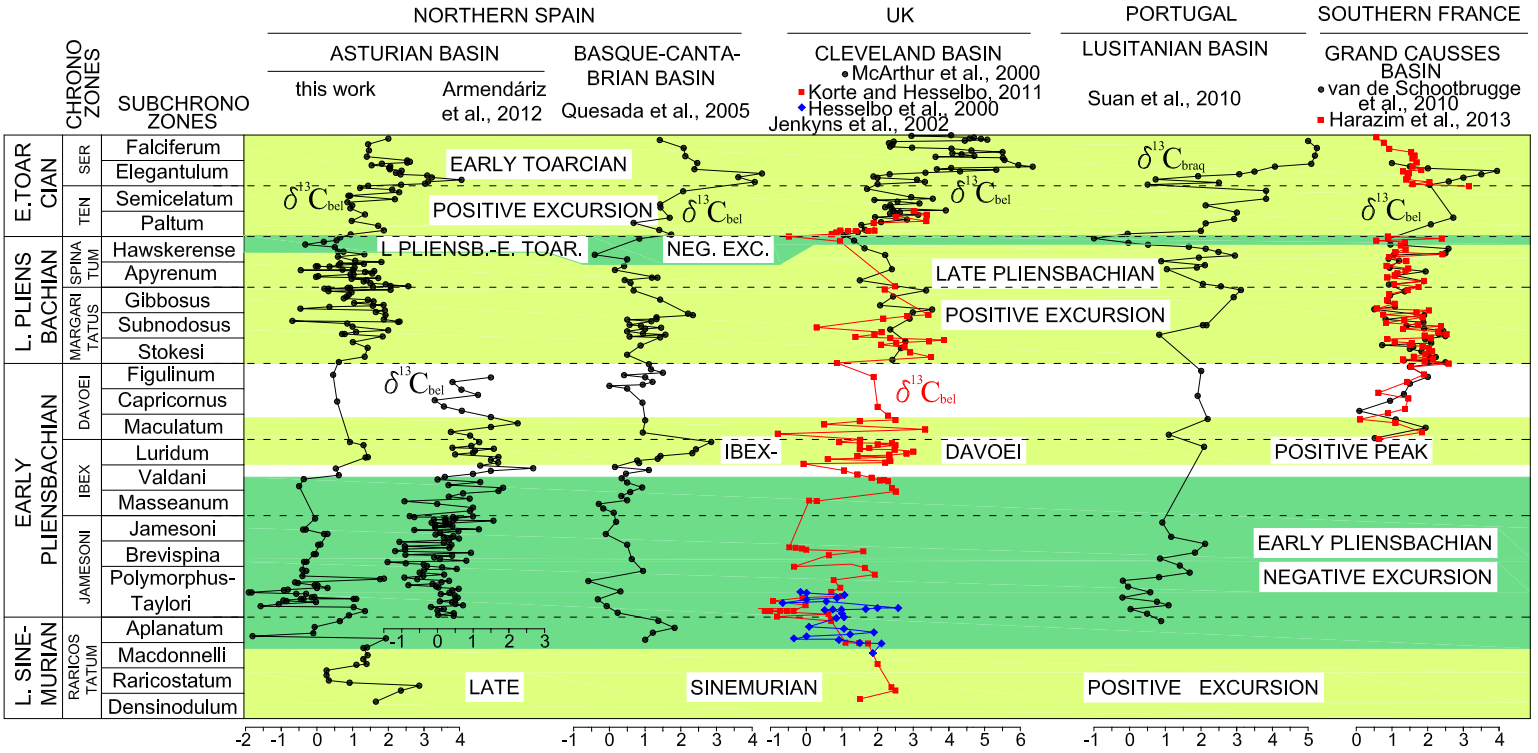

Fig. 6. Gómez, Comas-Rengifo and Goy

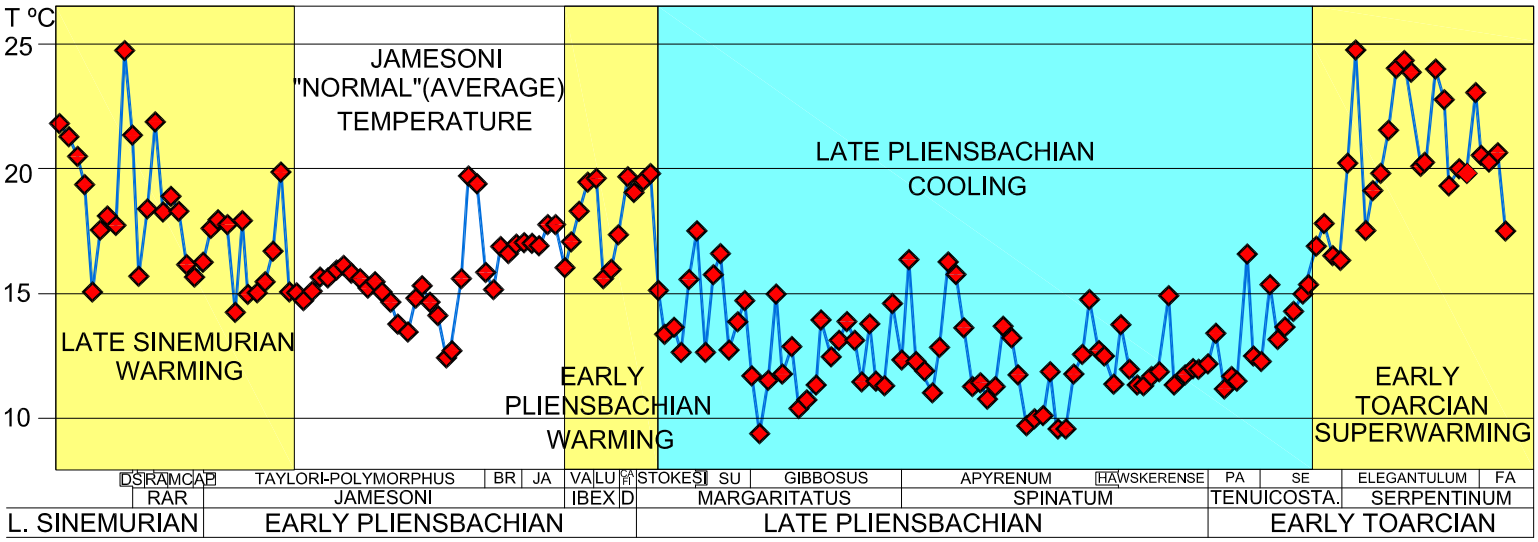

Fig. 7. Gómez, Comas-Rengifo and Goy

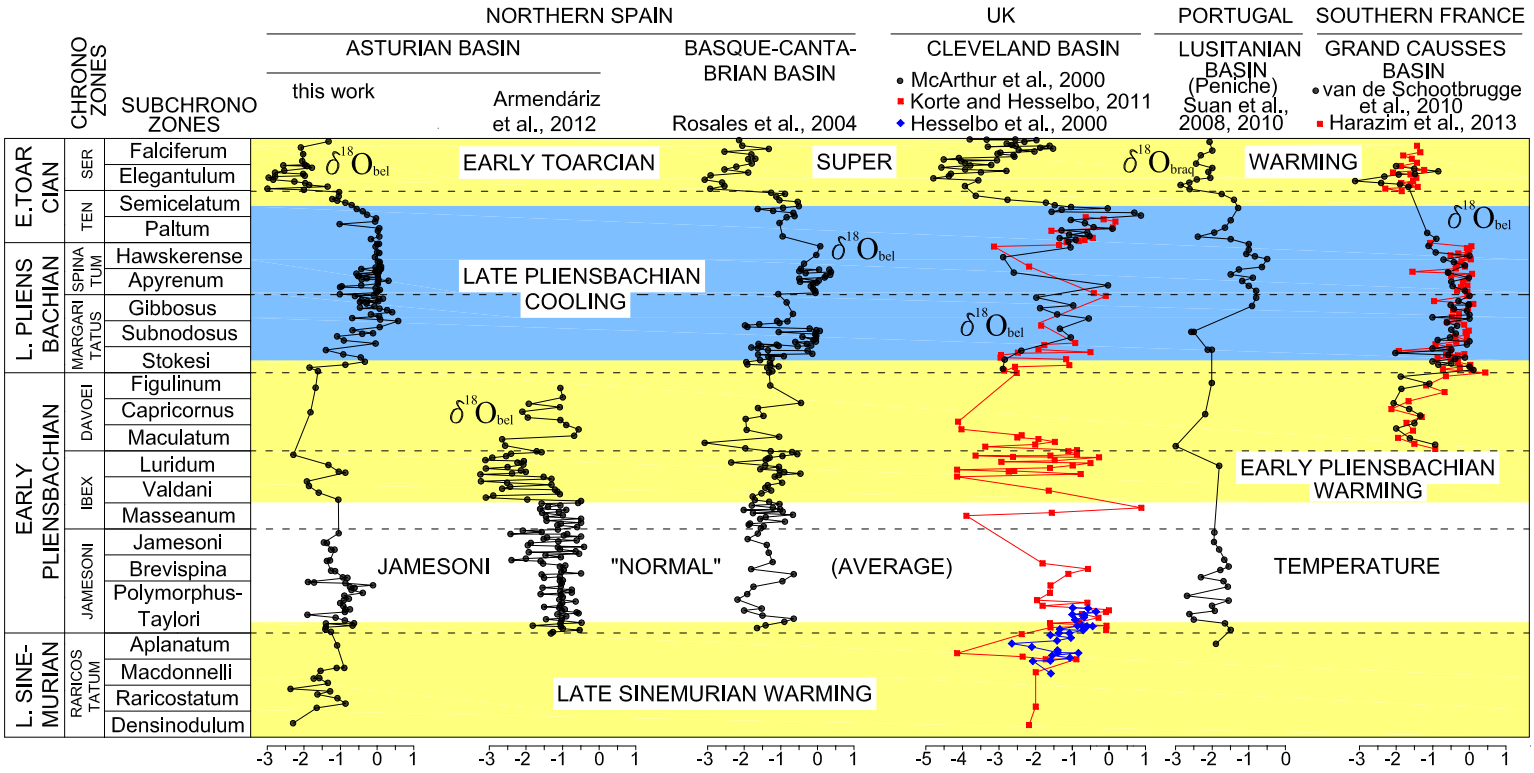

Fig. 8. Gómez, Comas-Rengifo and Goy